An introduction to applied quantum mechanics in the Wigner Monte Carlo formalism

J.M. Sellier [a,*], M. Nedjalkov [a,b], I. Dimov [a]

[a] IICT, Bulgarian Academy of Sciences, Acad. G. Bonchev str. 25A, 1113 Sofia, Bulgaria
[b] Institute for Microelectronics, TU Wien, Gußhausstraße 27-29/E360, 1040 Wien, Austria

ARTICLE INFO

ABSTRACT

The Wigner formulation of quantum mechanics is a very intuitive approach which allows the comprehension and prediction of quantum mechanical phenomena in terms of quasi-distribution functions. In this review, our aim is to provide a detailed introduction to this theory along with a Monte Carlo method for the simulation of time-dependent quantum systems evolving in a phase-space. This work consists of three main parts. First, we introduce the Wigner formalism, then we discuss in detail the Wigner Monte Carlo method and, finally, we present practical applications. In particular, the Wigner model is first derived from the Schrödinger equation. Then a generalization of the formalism due to Moyal is provided, which allows to recover important mathematical properties of the model. Next, the Wigner equation is further generalized to the case of many-body quantum systems. Finally, a physical interpretation of the negative part of a quasi-distribution function is suggested. In the second part, the Wigner Monte Carlo method, based on the concept of signed (virtual) particles, is introduced in detail for the single-body problem. Two extensions of the Wigner Monte Carlo method to quantum many-body problems are introduced, in the frameworks of time-dependent density functional theory and ab-initio methods. Finally, in the third and last part of this paper, applications to single- and many-body problems are performed in the context of quantum physics and quantum chemistry, specifically focusing on the hydrogen, lithium and boron atoms, the H_2 molecule and a system of two identical Fermions. We conclude this work with a discussion on the still unexplored directions the Wigner Monte Carlo method could take in the next future.

© 2015 Elsevier B.V. All rights reserved.

Contents

* Corresponding author.
  E-mail addresses: jeanmichel.sellier@parallel.bas.bg, jeanmichel.sellier@gmail.com (J.M. Sellier).

1. Introduction

The necessity of a quantum theory was raised by a series of experimental observations in the realm of extremely small objects such as electrons and other elementary particles, atoms and molecules, which could not be explained in classical terms at all. Concepts such as particle-wave duality and energy quantization have, indeed, no classical counterpart and the physical evidences for such phenomena were puzzling a whole community of scientists. Eventually, the remarkable (and stupendous) work assembled by the theoretical physicists of that time brought to a successful set of rules able to explain (and predict) the observed features of quantum systems. This achievement was in great part made possible thanks to the work of E. Schrödinger, summarizing the description of quantum systems in terms of probability amplitudes, or wave-functions, at that time a revolutionary concept. A physical interpretation to this equation was provided, known as the standard or Copenhagen interpretation. This theory remains, to this day, the most rigorously tested theory in physics.

Right after the birth of the Schrödinger equation, other formulations (and interpretations) of quantum mechanics appeared, shedding light on aspects that were hardly understandable in the standard formalism. In this perspective, the work of E. Wigner stands out among these alternative (but completely equivalent) formulations of quantum mechanics. Indeed it is an intuitive model which provides a direct connection between classical and quantum physics, due to its strong similarities with classical statistical mechanics. As a matter of fact, the Wigner approach renders quantum mechanics a more natural theory, describing quantum objects in terms of quasi-distribution functions.

Despite the advantage of being intuitive, only in recent years we have witnessed a growth of interest in the Wigner formulation of quantum mechanics. One plausible explanation for this is the fact that the Wigner equation has represented an incredibly challenging mathematical task for years, being a partial integro-differential equation where the unknown is a function defined over a $2 \times d \times n$ dimensional phase-space, where d is the dimensionality of space ($d = 1, 2, 3$) and n is the number of involved particles. Only recently, Monte Carlo techniques have been implemented which overcome the many problems involved in the resolution of such model.

In this review endeavor, the focal point will be the work of E. Wigner and the related Monte Carlo techniques which allow practical quantum simulations in the phase-space formulation. To this aim, we start this section by introducing some of the aspects of the necessity and birth of a quantum theory. Afterwards, we proceed with the tenets of the Schrödinger formalism and comment shortly on the Copenhagen interpretation. We, then, discuss on the role Monte Carlo methods have played in the field of applied physics and present the latest developments in the field of time-dependent, multi-dimensional and full

quantum simulations in the Wigner formalism. In the following we suppose the reader to be familiar with the Schrödinger formulation of quantum mechanics and the Dirac notation.

1.1. A short history of quantum mechanics

Quantum mechanics was born as a necessity to explain a series of experiments which are not understandable otherwise. Phenomena such as the black body radiation [1], the photo-electric effect [2] and the spectral lines of the hydrogen atom, just to mention some of the most typical examples, had no possible Newtonian explanation and were profoundly mining the validity of classical mechanics. Eventually, these experiments led to the birth of what is known today as the old quantum mechanics [3–5]. At that stage, the quantization of energy in systems was introduced phenomenologically and no rigorous justification was provided. A milestone in the early development of the new theory came with the work of E. Schrödinger who proposed his famous equation (1926) [6], describing quantum systems in terms of (complex) wave-functions $\psi = \psi(\mathbf{x})$. In his exposition, he was the first to propose a physical interpretation of the unknown function described by his equation, where he regarded the wave intensity $\psi^*\psi$ as the actual density of the electric charge. This approach was able to give a unique and independent image of the electron but was wrong. Indeed, being the Schrödinger equation linear, a charge would spread out very rapidly and without any limit. That is, of course, in contrast with the experimental evidence: indeed a particle is always found in a small region of space.

Subsequently, a heuristic interpretation of the wave-function in terms of *probability amplitudes* was given, known nowa-days as the *Born rule* (1926) [7]. In this explanation, the wave intensity is viewed as the *probability of finding a particle* rather than its density. In other words, the best possible description of a quantum system is of probabilistic nature. This interpre-tation was further developed by Bohr to the point that one should not even assign a meaning to precisely defined particle properties, such as position or velocity, beyond the limits specified by the Heisenberg uncertainty principle. According to this interpretation, no property has an independent existence. The Schrödinger equation and the Born rule, along with the following further prescriptions constitute what is, nowadays, known as the *standard* or *Copenhagen* interpretation of quan-tum mechanics: every system is completely represented by a wave-function $\psi(\mathbf{x}; t)$; when a measurement is performed, the wave-function collapses; the wave-particle duality of matter must be invoked to explain experimental results (Bohr complementarity principle); measuring devices are classical objects which can access only to classical properties. This is not the only possible interpretation of the Schrödinger equation and its interpretation still remains an open problem. As a matter of fact, many other conceivable interpretations exist [8–10].

Although the Schrödinger formalism is the *de-facto* standard, other possible approaches to quantum mechanics are available. Indeed, during its development, different but *mathematically equivalent* formulations have eventually been developed, with their respective advantages and disadvantages, among which we have the significant works of Wigner [11], Feynman [12] and Keldysh [13]. Interestingly enough, these approaches are not based on the concept of wave-functions, but on rather different mathematical objects such as quasi-distribution functions (Wigner), path integrals (Feynman), non-equilibrium Green functions (Keldysh), and still they provide the very same predictions as the Schrödinger equation. In a sense, the situation is not any different than classical mechanics where different, but mathematically equivalent, formalisms (such as Newtonian, Lagrangian, Hamiltonian, etc.) can be utilized to describe a system, depending on the mathematical convenience (a transform is always available to go from one formalism to another and vice versa).

The Wigner formalism has been successfully applied to problems related to nuclear physics [14–17], to the comprehen-sion of chemical reactions [18–24], and a thorough study on the quantum collision theory in this formalism has been carried out [25]. It is also a standard tool in the field of quantum optics [26]. More recently, the Wigner formalism has received a renewed attention from the scientific community and has been applied to new interesting physical problems. For example, it has been utilized to study the appearance of sub-Planck structures in phase-space which sheds light on the phenomenon of decoherence [27]. It is also worth to mention the recent studies performed in the field of nanoelectronics and nanotech-nology [28–33] completely based on the Wigner formalism (see also the pioneering works [34–36]). Finally, one should note that very recently the Wigner formalism has been extended to many-body problems in the frameworks of density functional theory (DFT) [37] and time-dependent ab-initio simulations [38]. It has shown to be a very convenient formalism when time-dependent, multi-dimensional and fully quantum simulations are necessary (see for example [39,40] and [41]).

In this work, we focus our attention on the Wigner formulation of quantum mechanics and show how to apply it for practical calculations related to quantum systems. As we will see throughout this review paper, the Wigner formalism is a very intuitive approach which describes quantum systems in terms of a quasi-distribution function $f_W = f_W(\mathbf{x}; \mathbf{p}; t)$, sometimes referred to as the Wigner function, where $(\mathbf{x}; \mathbf{p})$ is the corresponding phase-space, and $\mathbf{x} = (\mathbf{x}_1, \mathbf{x}_2, \ldots, \mathbf{x}_n)$ and $\mathbf{p} = (\mathbf{p}_1, \mathbf{p}_2, \ldots, \mathbf{p}_n)$ are the set of positions and the set of momenta of the involved particles respectively. We will show that, although the quasi-distribution function f_W can have negative values in some restricted region of the phase-space (where quantum effects are dominant), it can still be utilized as a regular distribution function to recover the value of macroscopic variables as is for the Boltzmann equation of classical statistical mechanics. As a matter of fact, the work of Wigner was first introduced as a quantum correction to classical thermodynamics. Thus, it is not surprising that the enunciation of Wigner is very close to the language of experimentalists, therefore putting quantum mechanics on relatively more reasonable foundations [42]. Finally, we will comment on the fact that today experimental techniques exist to measure the Wigner function and a convincing physical interpretation of the negative values of $f_W(\mathbf{x}; \mathbf{p}; t)$ can be given [43–45].

We now give a short introduction to the Monte Carlo method and its use in physics.

1.2. A (revised) history of Monte Carlo methods

The purpose of Monte Carlo methods is to approximate the solution of problems in computational mathematics by using random processes for each such problem. These methods give statistical estimates for any linear functional of the solution by performing random sampling of a certain random variable whose mathematical expectation is the desired functional [46]. Essentially, they reduce a given problem to approximate calculations of some mathematical expectation. They represent a very powerful tool when it comes to solve problems in mathematics, physics and engineering where the deterministic methods hopelessly break down. Indeed Monte Carlo methods do not require any additional regularity of the solution and it is always possible to control the accuracy of this solution in terms of the probability error. Another important advantage in using Monte Carlo methods consists in the fact that they are very efficient in dealing with large and very large computational problems such as multi-dimensional integration, very large linear systems, partial integro-differential equations in highly dimensional spaces, etc. Finally, these methods are efficient on parallel processors and parallel machines. Thus, it is not surprising that these methods have rapidly found a wide range of applications in applied Science.

Although the year 1949 is generally considered to be the official birthday of the Monte Carlo method [47], it is worth to note that earlier applications can be found in literature performed by the French mathematician Georges-Louis Leclerc, comte de Buffon in 1777 [48]. In his pioneering essay, known as *L'aiguille de Buffon* (Buffon's needle), he poses the following problem: supposing one drops a needle onto a floor made of parallel strips of wood (with the same width), what is the probability the needle lies across a line between two strips? He found that the solution is $\frac{2l}{\pi t}$, where l is the length of needle and t is the distance between each strip. As pointed out, later on, by Marquis Pierre-Simon de Laplace (in 1886), this approach can be used as a method to compute the value of the number π. As a matter of fact, by repeatedly throwing the needle onto a lined sheet of paper and counting the number of intersected lines, one can eventually estimate the value of π, in other words a Monte Carlo method to evaluate the number π. With the advent of computational resources, intensive applications started to be developed in the Manhattan project (Los Alamos, USA), by J. von Neumann, E. Fermi, G. Kahn and S.M. Ulam. The legend says that the name *Monte Carlo* was eventually suggested by N. Metropolis in honor of Ulam's uncle who was a well-known gambler.

With the development of even more powerful computers, especially parallel machines, a new momentum in the development of Monte Carlo methods has been provided. Indeed, nowadays, Monte Carlo algorithms exist to solve a plethora of different computational problems and it is practically impossible to specify a (even barely) complete list. Still, Monte Carlo methods can be divided into two main classes: *Monte Carlo simulations* and *Monte Carlo numerical methods*. In the first class, algorithms simulate physical processes and phenomena and these Monte Carlo methods are simply tools that mimic the corresponding physical, chemical or biological laws. A good example for this class is provided by the Boltzmann Monte Carlo method for the simulation of electron transport in semiconductor devices [49]. This algorithm reproduce the dynamics of a certain number of electrons which obey the law of classical physics when interacting with an external electric field (drift process) and behave quantum mechanically when interacting with the quantized lattice vibrations know as phonons (diffusion process). In the second class of Monte Carlo methods, we have instead stochastic numerical algorithms for the resolution of computational problems such as linear systems, eigenproblems, evaluation of multi-dimensional integrals, etc. These algorithms construct artificial random processes, usually Markovian, which mathematical expectation represents the solution of a given problem. A good example of such algorithms is given by the Monte Carlo method for linear systems discussed in [50].

In this review paper, we will focus only on a Monte Carlo method for the (time-dependent) solution of the Wigner equation. Recently several techniques to solve the Wigner equation have been developed which scale naturally on parallel machines, one being based on the concept of *particle quantum affinity* [28–31] (inspired by the pioneering works [51] and [52]), the other being based on the concept of *signed particles* on which we will mainly focus in this work [53,54]. The last method is based on the iterative Monte Carlo methods for the resolution of linear and non-linear systems of equations (both integral and algebraic) described in [50,55]. Very recently, the Wigner Monte Carlo method based on signed particles has open the way towards quantitative, time-dependent, multi-dimensional, single and many-body simulations in terms of affordable and reasonable computational resources. In practice, it has been applied to the simulation of quantum single-body problems in technologically relevant situations [39,40], extended to time-dependent quantum many-body problems in the framework of density functional theory [37], and has even been generalized to the ab-initio simulations of strongly correlated many-body problems [38]. This is the first time that the Wigner formalism can be applied to such class of important (and computationally demanding) problems. The authors believe this formalism and its related Monte Carlo method can have a profound impact in the field of applied Sciences, especially for physics and chemistry, since it offers a higher level of details in the simulation of quantum systems at a relatively reasonable computational cost. This is why, in the rest of the paper, we will mainly focus on the recent developments of the Wigner Monte Carlo method, its extensions to the quantum many-body problem, and its applications. We now introduce the Wigner formulation of quantum mechanics in detail.

2. Quantum mechanics in phase-space

The aim of this section is to introduce the main tenets of the Wigner formulation of quantum mechanics. To this purpose, we start from recalling the principle concepts of the Schrödinger approach. This is twofold. On the one hand, it establishes

the mathematical notation which will be utilized throughout this paper. On the other hand, the initial use of (standard) Schrödinger wave-functions enables a, somehow, quite natural approach to the Wigner formalism. Incidentally, the very first formulation of quantum mechanics in a phase-space was obtained as an attempt of E. Wigner to find quantum corrections to the Boltzmann equation of classical statistical physics [11] and was completely based on the concept of (pure state) wave-functions. A recent overview of the generalization of the work of Wigner to the case of mixed states was given in [56]. In this enunciation, the invariance of the Wigner equation with respect to the (anti-) symmetric wave-function defining the initial conditions is relatively simple to prove. We will make full use of this result to show how the Pauli exclusion principle is naturally embedded in the Wigner formalism [57]. Then, we proceed with sketching the work of J.E. Moyal [42], a generalization of the Wigner theory. This approach establishes elegant and convenient mathematical foundations for the Wigner model in both time-dependent and time-independent context and, furthermore, introduces the concept of stargenproblem (∗-genproblem). Along with the work of Dias and Prata [58], it depicts a quantum mechanical theory which is totally independent from the concept of wave-function. In particular, using the approach in [58], conditions to determine if a function defined over the phase-space has a physical meaning are established. Finally, the Wigner equation is generalized to the case of many-body particles. This will be useful when introducing the Monte Carlo techniques for time-dependent ab-initio simulations. To conclude, a short discussion about the connections between the Wigner quasi-distribution function and experimental observations is given, allowing the suggestion of a reasonable explanation of the negative values appearing in some area of the phase-space.

2.1. The Schrödinger formalism

The time-dependent and time-independent Schrödinger equations are two linear partial differential equations describing the state of a given quantum mechanical system [6]. Both have played a crucial role in the comprehension of Nature at a quantum level and can be considered the quantum analogues of Newton's second law. Nowadays, this approach is considered the standard in quantum mechanics. It is, thus, not surprising that E. Wigner utilized one of these equations (time-dependent) as a starting point to create his own formalism [11]. In this section we briefly recall the main tenets of the Schrödinger formulation of quantum mechanics. We adhere to the exposition of L.D. Landau [59] and limit ourselves to the non-relativistic case.

The Born rule. A (complex, normalized) wave-function $\psi = \psi(\mathbf{x})$ represents the most complete description of a given system which squared modulus $\psi^2(\mathbf{x})d\mathbf{x}$ is the probability of finding a particle around the position $\mathbf{x}$ in the interval $d\mathbf{x}$ (Born rule [7]).

Operators. To any physical quantity A, there is a corresponding Hermitian (linear) mathematical operator $\hat{A}$ which eigenvalues a_n are the possible outcomes of measuring A [59].

The time-independent Schrödinger equation. The time-independent Schrödinger equation is an eigenproblem which unknowns are the energy levels of a system along with the corresponding eigenfunctions. It describes quantum systems in the presence of time-independent external field and reads

$$\hat{H}\psi(\mathbf{x}) = E\psi(\mathbf{x}), \tag{1}$$

where $\hat{H}$ is known as the Hamiltonian operator and reads:

$$\hat{H} = \frac{\hat{p}^2}{2m} + U(\mathbf{x}) = -\frac{\hbar^2}{2m}\nabla_{\mathbf{x}}^2 + U(\mathbf{x}), \tag{2}$$

with m the mass of the particle and $U = U(\mathbf{x})$ the potential energy of the particle in an external field and the operator $\nabla_{\mathbf{x}}^2 = \frac{\partial^2}{\partial x^2} + \frac{\partial^2}{\partial y^2} + \frac{\partial^2}{\partial z^2}$.

The solution can be formally written as (E_n, ψ_n) for $n = 0, 1, 2, \ldots$, where the wave-functions ψ_n are also called stationary states, and the function ψ_0 and the energy E_0 are known as the *ground state* and the *zero-point energy* respectively. In particular, this equation implies the possibility for quantized energies.

The time-dependent Schrödinger equation. The time-dependent Schrödinger equation represents the most general description of a system in the wave-function formalism [6] and reads:

$$i\hbar\frac{\partial\psi(\mathbf{x};t)}{\partial t} = \hat{H}\psi(\mathbf{x};t). \tag{3}$$

One should note that being a *linear* partial differential equation, the principle of superposition holds.

2.2. The Wigner formalism

In 1932, in his search for quantum corrections to classical thermodynamic, E. Wigner came up with a very elegant and intuitive formulation of quantum mechanics in terms of phase-space and distribution functions [11]. In this section, we focus on the development of this formalism starting from the original work of Wigner in a pure quantum state. This approach is extended to the case of mixed states by exploiting the concept of density matrix. Then, we proceed with presenting the work

of J. Moyal which puts the theory on firm mathematical foundations. A study on the admissible states in the phase-space formulation, developed by Tatarskii, Prata and Dias, is presented, showing the (important) mathematical properties quasi-distribution functions must have in order to be valid descriptions of quantum systems and putting the Wigner theory on totally independent foundations with respect to the work of Schrödinger. Afterwards, we generalize the single-body Wigner equation to the quantum many-body case and to systems of identical particles (with a particular attention to Fermions). We conclude this section by commenting on a possible physical interpretation of the negative values appearing in quasi-distribution functions and its relation with experimental observations in quantum tomography.

2.2.1. Pure states

Assuming that the state of a single-body quantum system is represented by the wave-function $\psi(\mathbf{x}; t)$, it is possible to construct the following expression:

$$f_W(\mathbf{x}; \mathbf{p}; t) = \frac{1}{(\hbar\pi)^d} \int_{-\infty}^{+\infty} d\mathbf{x}' \psi^*(\mathbf{x} + \mathbf{x}'; t) \psi(\mathbf{x} - \mathbf{x}'; t) e^{-\frac{2i}{\hbar}\mathbf{x}'\cdot\mathbf{p}}, \tag{4}$$

(we remind that $d = 1, 2, 3$ is the dimension of the spatial domain). It can be shown that the function $f_W = f_W(\mathbf{x}; \mathbf{p}; t)$ is real but not positive definite [11], thus it cannot be considered a proper distribution function. However this function has convenient and useful mathematical properties: when integrated with respect to $\mathbf{p}$ it gives the quantity

$$\int_{-\infty}^{+\infty} d\mathbf{p} f_W(\mathbf{x}; \mathbf{p}; t) = |\psi(\mathbf{x}; t)|^2,$$

which represents the probability of finding the particle in a certain position, while when integrated with respect to $\mathbf{x}$ it gives the probability for the momentum, i.e.

$$\int_{-\infty}^{+\infty} d\mathbf{x} f_W(\mathbf{x}; \mathbf{p}; t) = \left| \int d\mathbf{x} \psi(\mathbf{x}; t) e^{-\frac{i}{\hbar}\mathbf{x}\cdot\mathbf{p}} \right|^2.$$

Accordingly, it follows that one can calculate the space-dependent and space-independent expectation values $\bar{A}(\mathbf{x})$ and $\langle A \rangle$ of any function (macroscopic variable) of coordinates and momenta $A = A(\mathbf{x}; \mathbf{p})$, i.e.

$$\bar{A}(\mathbf{x}) = \int_{-\infty}^{+\infty} d\mathbf{p} A(\mathbf{x}; \mathbf{p}) f_W(\mathbf{x}; \mathbf{p}; t), \tag{5}$$

and

$$\langle A \rangle = \int_{-\infty}^{+\infty} d\mathbf{x} \bar{A}(\mathbf{x}) = \int_{-\infty}^{+\infty} \int_{-\infty}^{+\infty} d\mathbf{x} d\mathbf{p} A(\mathbf{x}; \mathbf{p}) f_W(\mathbf{x}; \mathbf{p}).$$

Therefore, it follows that despite the function f_W is a quasi-distribution function it can still be utilized in practical situations for the calculation of the average values $\langle A \rangle$ and $\bar{A}(\mathbf{x})$ of a given macroscopic variable $A(\mathbf{x}; \mathbf{p})$. Yet the quantity $f_W(\mathbf{x}; \mathbf{p}; t)$ cannot be interpreted as a simultaneous probability for both position and momentum of a particle (despite they are independent variables).

Exploiting the fact that the wave-function $\psi(\mathbf{x}; t)$ evolves according to the time-dependent Schrödinger equation (3), it is possible to derive the corresponding evolution equation for the quasi-distribution function $f_W(\mathbf{x}; \mathbf{p}; t)$. Indeed, by making use of the definition (4), it is possible to calculate the time derivative of the function $f_W(\mathbf{x}; \mathbf{p}; t)$ [11]:

$$\frac{\partial f_W}{\partial t}(\mathbf{x}; \mathbf{p}; t) = \frac{1}{(\hbar\pi)^d} \frac{\partial}{\partial t} \int_{-\infty}^{+\infty} d\mathbf{x}' \psi^*(\mathbf{x} + \mathbf{x}'; t) \psi(\mathbf{x} - \mathbf{x}'; t) e^{\frac{2i}{\hbar}\mathbf{x}'\cdot\mathbf{p}}$$

$$= \frac{1}{(\hbar\pi)^d} \int_{-\infty}^{+\infty} d\mathbf{x}' e^{\frac{2i}{\hbar}\mathbf{x}'\cdot\mathbf{p}} \left[\frac{\partial\psi^*}{\partial t}(\mathbf{x} + \mathbf{x}'; t) \psi(\mathbf{x} - \mathbf{x}'; t) + \psi^*(\mathbf{x} + \mathbf{x}'; t) \frac{\partial\psi}{\partial t}(\mathbf{x} - \mathbf{x}'; t) \right], \tag{6}$$

where, from (3) one has:

$$\frac{\partial\psi}{\partial t}(\mathbf{x} - \mathbf{x}'; t) = \frac{1}{i\hbar} \left[-\frac{\hbar^2 \nabla_{\mathbf{x}}^2 \psi(\mathbf{x} - \mathbf{x}'; t)}{2m} + U(\mathbf{x} - \mathbf{x}'; t) \psi(\mathbf{x} - \mathbf{x}'; t) \right]. \tag{7}$$

Furthermore, from the complex conjugate of (3) one has:

$$\frac{\partial\psi^*}{\partial t}(\mathbf{x} + \mathbf{x}'; t) = \frac{1}{i\hbar} \left[\frac{\hbar^2 \nabla_{\mathbf{x}}^2 \psi^*(\mathbf{x} + \mathbf{x}'; t)}{2m} - U(\mathbf{x} + \mathbf{x}'; t) \psi^*(\mathbf{x} + \mathbf{x}'; t) \right]. \tag{8}$$

Thus, by substituting (7) and (8) into (6), replacing the differentiations with respect to $\mathbf{x}$ by differentiations with respect to $\mathbf{x}'$, and performing partial integrations for the terms containing the operator $\nabla_{\mathbf{x}}^2$, one can easily show that [11]:

$$
\frac{\partial f_W}{\partial t}(\mathbf{x}; \mathbf{p}; t) = \frac{1}{(\hbar\pi)^d} \int_{-\infty}^{+\infty} d\mathbf{x}' e^{\frac{2i}{\hbar}\mathbf{x}'\cdot\mathbf{p}}
$$
$$
\cdot \left\{ \frac{\mathbf{p}}{m} \left[-\nabla_{\mathbf{x}'}\psi^*(\mathbf{x}+\mathbf{x}'; t)\psi(\mathbf{x}-\mathbf{x}'; t) + \nabla_{\mathbf{x}'}\psi(\mathbf{x}-\mathbf{x}'; t)\psi^*(\mathbf{x}+\mathbf{x}'; t) \right] \right.
$$
$$
\left. + \psi^*(\mathbf{x}+\mathbf{x}'; t)\psi(\mathbf{x}-\mathbf{x}'; t) \left[U(\mathbf{x}+\mathbf{x}'; t) - U(\mathbf{x}-\mathbf{x}'; t) \right] \right\},
\tag{9}
$$

from which (by replacing the differentiations with respect to $\mathbf{x}'$ back to $\mathbf{x}$) one finally obtains the (time-dependent) Wigner equation:

$$
\frac{\partial f_W}{\partial t} + \frac{\mathbf{p}}{m}\cdot\nabla_{\mathbf{x}}f_W = \int_{-\infty}^{+\infty} d\mathbf{p}' V_W(\mathbf{x}; \mathbf{p}'; t)f_W(\mathbf{x}; \mathbf{p}+\mathbf{p}'; t),
\tag{10}
$$

where

$$
V_W(\mathbf{x}; \mathbf{p}; t) = \frac{i}{\pi^d\,\hbar^{d+1}} \int d\mathbf{x}' e^{-\left(\frac{i}{\hbar}\right)\mathbf{x}'\cdot\mathbf{p}} \left[U\left(\mathbf{x}+\frac{\mathbf{x}'}{2}; t\right) - U\left(\mathbf{x}-\frac{\mathbf{x}'}{2}; t\right) \right],
\tag{11}
$$

referred to as the *Wigner kernel* (or, sometimes, the *Wigner potential*) and where the external potential $U = U(\mathbf{x}; t)$ can be varying in time.

Eq. (10) is known as the *Wigner equation* and describes the dynamics of a system consisting of a single particle in the presence of an external potential $U(\mathbf{x}; t)$. This equation is of paramount importance in the Wigner formulation of quantum mechanics and will be the focus of this review effort. The Wigner equation (10) represents what the Schrödinger equation (3) represents in the standard formalism (indeed in the next section we show that they are mathematically equivalent). It is a statistical approach to quantum mechanics, although not in a classical sense as the function f_W can have negative values. Unlike classical statistics which can be regarded as a *crypto-deterministic* theory and the whole uncertainty of a system is contained in the initial conditions, in the Wigner approach the time evolution of f_W is not necessarily crypto-deterministic (in a classical sense at least) [42]. Moreover, the definition (11) gives an important insight as it shows the quantum mechanical nature of the quasi-distribution f_W. Indeed, one possible interpretation of the kernel $V_W(\mathbf{x}; \mathbf{p}; t)$ is given in [11]: V_W represents the probability for a particle to jump in the phase-space and have a momentum $\mathbf{p}$; this jump happens discontinuously and in discrete amounts equivalent to half the momenta of light quanta, as if the potential were composed of light.

Finally, it is important to note that if the potential $U = U(\mathbf{x}; t)$ can be developed in a Taylor series, then the Wigner equation (10) reads:

$$
\frac{\partial f_W}{\partial t} + \frac{\mathbf{p}}{m}\cdot\nabla_{\mathbf{x}}f_W - \nabla_{\mathbf{x}}U\cdot\nabla_{\mathbf{p}}f_W = \sum_{l=1}^{+\infty} \frac{(-1)^l}{(2l)!}\left(\frac{\hbar}{2}\right)^{2l}\nabla_{\mathbf{x}}^{2l}U\cdot\nabla_{\mathbf{p}}^{2l}f_W,
\tag{12}
$$

where, in a three-dimensional space, $\nabla_{\mathbf{x}}^{2l} = \left(\frac{\partial^{2l}}{\partial x^{2l}}, \frac{\partial^{2l}}{\partial y^{2l}}, \frac{\partial^{2l}}{\partial z^{2l}}\right)$, $\nabla_{\mathbf{p}}^{2l} = \left(\frac{\partial^{2l}}{\partial p_x^{2l}}, \frac{\partial^{2l}}{\partial p_y^{2l}}, \frac{\partial^{2l}}{\partial p_z^{2l}}\right)$ with $\mathbf{x} = (x, y, z)$ and $\mathbf{p} = (p_x, p_y, p_z)$. In particular, one easily observes that in the limiting case $\hbar \to 0$ the Wigner equation (12) reduces to:

$$
\frac{\partial f}{\partial t} + \frac{\mathbf{p}}{m}\cdot\nabla_{\mathbf{x}}f - \nabla_{\mathbf{x}}U\cdot\nabla_{\mathbf{p}}f = 0,
\tag{13}
$$

which is known as the Vlasov equation (or the Boltzmann equation in the ballistic case) and describes a classical system in terms of a distribution function $f = f(\mathbf{x}; \mathbf{p}; t)$ (i.e. non-negative definite). Thus, the emergence of classical mechanics from quantum mechanics can be easily explained in this context. Additionally, one should note that when the potential $U(\mathbf{x})$ can be expressed as a polynomial of second order, it is easy to prove that the Wigner equation (12) reduces again to the Vlasov equation (13), which solution can be found analytically by means of the method of characteristics (for the case of a time-independent potential, the Vlasov equation reduces to a scalar hyperbolic equation).

2.2.2. Mixed states

When conducting an experiment, it is not always possible to know which quantum state is currently being manipulated. This situation arises, for example, in systems in thermal equilibrium or in systems with a random preparation history. In this case, the pure state approach depicted in Eqs. (1) and (3) is not useful any longer and the concept of *density matrix* is more suitable. In the following, we use the mathematical approach described in [56] and we show that the evolution equation for the Wigner function remains unchanged.

In the coordinate representation, the density matrix $\rho(\mathbf{x}; \mathbf{x}'; t)$ is defined as:

$$
\rho(\mathbf{x}; \mathbf{x}'; t) = \sum_i p_i \psi(\mathbf{x}; t)\psi^*(\mathbf{x}'; t),
\tag{14}
$$

where p_i is the statistical weight of the pure (normalized) state $\psi(\mathbf{x})$. The corresponding evolution equation, known as the Liouville–von Neumann equation (or the Von Neumann equations *tout court*), was depicted for the first time by J. von Neumann [60] and reads:

$$i\hbar \frac{\partial \rho}{\partial t} = \left[\hat{H}, \rho\right],$$
(15)

where the brackets $[., .]$ denote the commutator $[X, Y] = XY - YX$. Now, by exploiting the definition of a macroscopic variable (5), it is possible to express the Wigner quasi-distribution function $f_W(\mathbf{x}; \mathbf{p}; t)$ in terms of the density matrix $\rho(\mathbf{x}; \mathbf{x}')$ [56]:

$$f_W(\mathbf{x}; \mathbf{p}; t) = \frac{1}{(\pi\hbar)^d} \int d\mathbf{x}' \rho(\mathbf{x} - \mathbf{x}'; \mathbf{x} + \mathbf{x}'; t) e^{\frac{2i}{\hbar}\mathbf{x}' \cdot \mathbf{p}}.$$
(16)

By applying the transform (16) to Eq. (15), it is possible to show that the evolution equation for the Wigner function corresponding to the mixed state regime essentially remains the same as (10) [56]. In other words, despite the mixed states definition (16) differs from the pure state definition (4), the evolution equation does not change. This is certainly not surprising if one reminds that the density matrix is a combination of pure states and the Wigner function is a bilinear combination of these states.

2.3. The Wigner formalism for the many-body problem

In this section, we introduce the time-dependent quantum many-body problem for an arbitrary number n of particles in the Wigner formalism. At a first glance, this formulation does not seem to introduce any particular advantage over the standard approach, as the mathematical expressions involved are incredibly complicated. But later we will see that, thanks to the Monte Carlo techniques nowadays available, the Wigner formalism actually brings an important pool of possibilities which are hardly imaginable in other formulations of quantum mechanics.

We show that a many-body quasi-distribution function can be defined for such systems and an evolution equation can be delineated. For the sake of clarity and completeness, we start from describing the problem in the Schrödinger formalism. Then we introduce the many-body Wigner equation. Finally we conclude by discussing the simulation of systems of indistinguishable particles in the phase-space quantum theory.

2.3.1. The many-body Schrödinger and von Neumann equations

In the presence of a quantum system composed of n interacting particles, a time-dependent Schrödinger equation similar to (3) can be depicted. In particular, the space of configurations now consists of the coordinates of n particles, and is denoted as

$$\mathbf{x} = (\mathbf{x}_1, \mathbf{x}_2, \ldots, \mathbf{x}_n),$$
(17)

where $\mathbf{x}_i = (x_i, y_i, z_i)$ are the spatial coordinates of the ith particle, and $i = 1, 2, \ldots, n$. Accordingly, the wave-function is a function of the n-body configuration space and the many-body time-dependent Schrödinger equation reads

$$i\hbar \frac{\partial \psi}{\partial t}(\mathbf{x}_1, \mathbf{x}_2, \ldots, \mathbf{x}_n; t) = \hat{H}\psi(\mathbf{x}_1, \mathbf{x}_2, \ldots, \mathbf{x}_n; t),$$
(18)

where the Hamiltonian operator $\hat{H}$ is generalized as

$$\hat{H} = \hat{H}\left(\hat{\mathbf{x}}_1, \hat{\mathbf{x}}_2, \ldots, \hat{\mathbf{x}}_n; \hat{\mathbf{p}}_1, \hat{\mathbf{p}}_2, \ldots, \hat{\mathbf{p}}_n\right)$$
$$= -\sum_{i=1}^{n} \frac{\hat{\mathbf{p}}_i^2}{2m} + U(\mathbf{x}_1, \mathbf{x}_2, \ldots, \mathbf{x}_n; t),$$
(19)

with $\hat{\mathbf{x}}_i = (\hat{x}_i, \hat{y}_i, \hat{z}_i)$ and $\hat{\mathbf{p}}_i = -i\hbar\nabla_i = -i\hbar\left(\frac{\partial}{\partial x_i}, \frac{\partial}{\partial y_i}, \frac{\partial}{\partial z_i}\right)$ the position and momentum operators for the ith particle respectively.

In the same way, the Liouville–von Neumann equation is modified to take into account the many-body configuration space. In this context, this equation now reads:

$$\frac{\partial \rho}{\partial t}(\mathbf{x}_1, \mathbf{x}_2, \ldots, \mathbf{x}_n) = \frac{1}{i\hbar}\left[H\left(\hat{\mathbf{x}}_1, \hat{\mathbf{x}}_2, \ldots, \hat{\mathbf{x}}_n; \hat{\mathbf{p}}_1, \hat{\mathbf{p}}_2, \ldots, \hat{\mathbf{p}}_n\right), \rho(\mathbf{x}_1, \mathbf{x}_2, \ldots, \mathbf{x}_n)\right],$$
(20)

which can be seen as a generalization of the single-body Liouville–von Neumann (15), with the operator $\hat{H}$ as in (20). One should note that despite the mathematical structure of the many-body Eq. (20) is essentially the same as Eq. (15), this equation represents an incredibly more complex mathematical challenge, even when approached by numerical techniques. The same applies to the many-body Schrödinger equation as both models are defined over a $n \cdot d$-dimensional configuration space.

2.3.2. The many-body Wigner equation

The Wigner formulation of quantum mechanics allows the description of systems consisting of n interacting particles by means of a quasi-distribution function $f_W = f_W(\mathbf{x}; \mathbf{p}; t)$, where the phase-space is now a $2 \cdot n \cdot d$-dimensional space $(\mathbf{x}; \mathbf{p}) = (\mathbf{x}_1, \mathbf{x}_2, \ldots, \mathbf{x}_n; \mathbf{p}_1, \mathbf{p}_2, \ldots, \mathbf{p}_n)$, where $\mathbf{x}_i$ and $\mathbf{p}_i$ have the usual meaning. In this new context, the pure state Wigner function reads:

$$f_W(\mathbf{x}; \mathbf{p}; t) = \frac{1}{(\hbar\pi)^{d \cdot n}} \int d\mathbf{x}' e^{-\frac{i}{\hbar} \sum\limits_{k=1}^{n} \mathbf{x}'_k \cdot \mathbf{p}_k} \times \Psi\left(\mathbf{x} + \frac{\mathbf{x}'}{2}; t\right) \Psi^*\left(\mathbf{x} - \frac{\mathbf{x}'}{2}; t\right), \tag{21}$$

where $\Psi = \Psi(\mathbf{x}; t)$ is a Schrödinger many-body pure state, $\int d\mathbf{x}' = \int d\mathbf{x}'_1 \int d\mathbf{x}'_2 \cdots \int d\mathbf{x}'_n$, and $(\mathbf{x} \pm \frac{\mathbf{x}'}{2}) = (\mathbf{x}_1 \pm \frac{\mathbf{x}'_1}{2}, \mathbf{x}_2 \pm \frac{\mathbf{x}'_2}{2}, \ldots, \mathbf{x}_n \pm \frac{\mathbf{x}'_n}{2}; t)$. Analogously, a definition can be given in case of mixed states described by a many-body density matrix $\rho = \rho(\mathbf{x}; \mathbf{y}; t)$

$$f_W(\mathbf{x}; \mathbf{p}; t) = \frac{1}{(\hbar\pi)^{d \cdot n}} \int d\mathbf{x}' e^{-\frac{i}{\hbar} \sum\limits_{k=1}^{n} \mathbf{x}'_k \cdot \mathbf{p}_k} \rho\left(\mathbf{x} + \frac{\mathbf{x}'}{2}; \mathbf{x} - \frac{\mathbf{x}'}{2}; t\right). \tag{22}$$

By applying the transform (21) to the many-body Schrödinger equation (18), one obtains the corresponding time-dependent many-body Wigner equation:

$$\frac{\partial f_W}{\partial t}(\mathbf{x}; \mathbf{p}; t) + \sum_{k=1}^{n} \frac{\mathbf{p}_k}{m_k} \cdot \nabla_{\mathbf{x}_k} f_W = \int d\mathbf{p} f_W(\mathbf{x}; \mathbf{p}; t) V_W(\mathbf{x}; \mathbf{p}; t), \tag{23}$$

where $\int d\mathbf{p} = \int d\mathbf{p}_1 \int d\mathbf{p}_2 \cdots \int d\mathbf{p}_n$, m_k is the mass of the kth particle, and the many-body Wigner kernel $V_W = V_W(\mathbf{x}; \mathbf{p}; t)$, now reads:

$$V_W(\mathbf{x}; \mathbf{p}; t) = \frac{i}{\pi^{dn} \hbar^{dn+1}} \int d\mathbf{x}' e^{-\left(\frac{2i}{\hbar}\right) \sum\limits_{k=1}^{n} \mathbf{x}'_k \cdot \mathbf{p}_k} \left[U\left(\mathbf{x} + \frac{\mathbf{x}'}{2}; t\right) - U\left(\mathbf{x} + \frac{\mathbf{x}'}{2}; t\right) \right]. \tag{24}$$

The function $U = U(\mathbf{x}; t) = U(\mathbf{x}_1, \mathbf{x}_2, \ldots, \mathbf{x}_n)$ is the potential acting over the n particles, and, in general, can vary in time and further details are provided in the next section.

2.3.3. Notes on the many-body potential

Usually, the potential $U = U(\mathbf{x})$ is expressed as a sum of two terms

$$U(\mathbf{x}) = V_{ext}(\mathbf{x}) + V_{ee}(\mathbf{x}) \tag{25}$$

where $V_{ext}(\mathbf{x})$ and $V_{ee}(\mathbf{x})$ represent the external and electron–electron interaction potentials. More specifically, the term V_{ext} most commonly describes either an external potential applied to the system, such as one obtained by connecting leads providing an applied electrostatic potential (typical in the simulation of electron transport in electronic devices) or the potential due the nuclei (if a molecular system is studied). The term V_{ee} represents, instead, the inclusion of electron–electron electrostatic interactions due to their Coulombic potential. Usually, this term is given by the Hartree approximation (in atomic units):

$$V_{ee}(\mathbf{x}) = \frac{1}{2} \sum_{i \neq j}^{n} \frac{e^2}{|\mathbf{x}_i - \mathbf{x}_j|}, \tag{26}$$

with e the elementary charge. In particular, for an isolated molecular system one has:

$$U(\mathbf{x}; t) = -\sum_{i,j=1}^{n_{ion}} \frac{Z_j e^2}{|\mathbf{x}_i - \mathbf{x}_j|} + \frac{1}{2} \sum_{i \neq j}^{n} \frac{e^2}{|\mathbf{x}_i - \mathbf{x}_j|}, \tag{27}$$

where the first term represents the superposition of Coulombic potentials due to the nuclei (which atomic number is Z_j for the jth nucleus).

2.3.4. Identical particles

A very interesting case for applied quantum physics and quantum chemistry is represented by systems consisting of *indistinguishable Fermions*. In order to treat this case in the many-body Wigner formalism, we follow the reasoning reported in [56]. In a previous section, we have shown that, starting from the many-body Liouville–von Neumann equation (20), and by applying the transform (22) to it, one recovers the many-body Wigner equation (23). One should note that, in the process, no assumption has been made on the symmetry properties of the system [56].

Now, it is well known that indistinguishable Fermions in the standard formalism are described by antisymmetric wave-functions, i.e.

$$\Psi(\mathbf{x}_1, \mathbf{x}_2, \ldots, \mathbf{x}_i, \ldots, \mathbf{x}_j, \ldots, \mathbf{x}_n; t) = -\Psi(\mathbf{x}_1, \mathbf{x}_2, \ldots, \mathbf{x}_j, \ldots, \mathbf{x}_i, \ldots, \mathbf{x}_n; t). \tag{28}$$

Therefore, taking into account the antisymmetric nature of the system, one can define a Weyl map for Fermions

$$f_W^-(\mathbf{x}; \mathbf{p}; t) = \frac{1}{(\hbar\pi)^{d\cdot n}} \int d\mathbf{x}' e^{-\frac{i}{\hbar}\sum_{k=1}^{n}\mathbf{x}'_k\cdot\mathbf{p}_k} \times \Psi^-\left(\mathbf{x}_1 + \frac{\mathbf{x}'_1}{2}, \ldots, \mathbf{x}_n + \frac{\mathbf{x}'_n}{2}; t\right)$$

$$\times \Psi^{-*}\left(\mathbf{x}_1 - \frac{\mathbf{x}'_1}{2}, \ldots, \mathbf{x}_n - \frac{\mathbf{x}'_n}{2}; t\right), \tag{29}$$

where $\Psi^-(\mathbf{x}_1, \ldots, \mathbf{x}_n)$ is an antisymmetric many-body wave-function. The case for mixed states is obtained in a similar way in [56]. It is possible to show that the many-body Wigner equation for indistinguishable Fermions is again (23) [56,61]. Indeed, the outcome of applying the transform (22) to Eq. (20) does not depend on the symmetry properties of the system. This proves that the whole Wigner formalism does not need any change to treat the case of antisymmetric systems [56]. In particular, an important point is that the Pauli exclusion principle is directly embedded into the Wigner formalism and does not necessitate to be imposed.

As a consequence, the antisymmetric properties of the system are defined through the initial conditions only. Thus, in order to handle systems of Fermions, one simply starts from a Slater determinant imposed at a initial time, say $t = 0$:

$$\Psi^-(\mathbf{x}_1, \ldots, \mathbf{x}_n) = \frac{1}{\sqrt{n!}} \begin{vmatrix} \phi_1(\mathbf{x}_1) & \phi_2(\mathbf{x}_1) & \ldots & \phi_n(\mathbf{x}_1) \\ \phi_1(\mathbf{x}_2) & \phi_2(\mathbf{x}_2) & \ldots & \phi_n(\mathbf{x}_2) \\ \ldots & \ldots & \ldots & \ldots \\ \phi_1(\mathbf{x}_n) & \phi_2(\mathbf{x}_n) & \ldots & \phi_n(\mathbf{x}_n) \end{vmatrix}, \tag{30}$$

(although the reader should note that this is not the only possible choice). It can be shown that this is equivalent to express the initial Wigner function as a sum of reduced single-particle Wigner functions and a number of integral terms [62,63]. As a matter of fact, this couples the involved Fermions together, in agreement with the fact that the corresponding initial Wigner function cannot be expressed as multiplications of independent wave-packets only.

2.4. The Moyal formalism

In 1949 J. Moyal published an important contribution to the theory of quantum mechanics in phase-space. In a brilliant attempt to understand if the Wigner approach was a proper statistical theory, he merged the works of E. Wigner [11], J. von Neumann [60], H. Weyl [64] and H. Groenewold [65] in a elegant and firm mathematical framework [42]. This formulation is statistical and provides a way to connect classical mechanics to quantum mechanics, allowing a natural comparison between these drastically different theories of Nature. Moreover, the work of Moyal allows to completely avoid the use of operators for observables, a very intuitive perspective especially if compared to the standard approach of quantum mechanics. In the following, for simplicity we introduce the theory for the one-dimensional space, being the generalization to higher dimensional spaces trivial.

The Weyl map. A fundamental mathematical tool in the Moyal theory is represented by the Weyl map. The Weyl map M_W, also known as the Weyl correspondence rule or the Wigner–Weyl transform, is an isomorphism from the space of linear operators $\hat{A}$ with a product $\cdot$ and a commutator $[., .]$ to the space of functions $A(x; p)$ defined over the phase-space with a (non-commutative) product $*$, known as the Groenewold product [65] and bracket $[., .]_M$, known as the Moyal bracket [42]:

$$\left(\hat{A}\left(\hat{x}; \hat{p}\right), \cdot, [., .]\right) \rightarrow \left(A(x; p), *, [., .]_M\right).$$

In particular, given a quantum operator $\hat{A} = \hat{A}\left(\hat{x}; \hat{p}\right)$, expressed in terms of the position and momentum operators $\hat{x}$ and $\hat{p}$ respectively, the Weyl map is mathematically defined as:

$$M_W\left(\hat{A}\right)(x; p) = A(x; p) = \frac{\hbar}{2\pi} \int d\xi \int d\eta Tr\left[\hat{A}\left(\hat{x}; \hat{p}\right)e^{i(\xi\hat{x}+\eta\hat{p})}\right]e^{-i(\xi x+\eta p)}, \tag{31}$$

where $Tr[.]$ is the trace of an operator and the exponential of an operator is defined as $e^{\hat{X}} = \sum_{l=0}^{+\infty}\frac{1}{l!}\hat{X}^l$. An important property of the Wigner mapping is that it is invertible [58]. The Groenewold $*$-product and Moyal bracket $[., .]$ can be defined in terms of the Weyl map. As a matter of fact, given two operators $\hat{A}$ and $\hat{B}$ which corresponding Weyl transforms are the functions $A = A(x; p)$ and $B = B(x; p)$ one has:

$$A * B = M_W\left(\hat{A}, \hat{B}\right) \tag{32}$$

$$[A, B]_M = \frac{1}{i\hbar}(A * B - B * A) = \frac{1}{i\hbar}M_W\left(\left[\hat{A}, \hat{B}\right]\right). \tag{33}$$

In this formalism, the Wigner quasi-distribution function is defined as the Weyl transform of the density matrix operator times a normalization factor, i.e.:

$$f_W(x; p; t) = \frac{1}{2\pi\hbar} M_W(\hat{\rho}(t)),$$ (34)

and, for the particular case of pure states, it is possible to show that [58]:

$$\begin{aligned} f_W(x; p; t) &= \frac{1}{2\pi} \int dy\, \psi^*\left(x + \frac{\hbar y}{2}; t\right) \psi\left(x - \frac{\hbar y}{2}; t\right) e^{-iyp} \\ &= \frac{1}{\hbar\pi} \int dx'\, \psi^*(x + x'; t) \psi(x - x'; t) e^{-\frac{2i}{\hbar} x' \cdot p}, \end{aligned}$$

i.e. formula (4). One can also show that the function $f_W(x; p; t)$ is square integrable, normalized and real, but not positive defined.

2.4.1. Evolution equations

The time-independent equation. One important point of the work of Moyal is represented by the so-called $*$-genproblem, essentially corresponding to the time-independent Schrödinger equation in the Wigner formalism. If an operator $\hat{A}$ is given with a non-degenerate spectrum and, in the Dirac notation, $|a\rangle$ is one of its eigenvectors corresponding to the eigenvalue a, i.e.

$$\hat{A}|a\rangle = a|a\rangle,$$

then it is possible to show that the corresponding Wigner function, defined as $f_W^a(x; p) = \frac{1}{2\pi\hbar} V_W(|a\rangle\langle a|)$, is the solution of the following problem [42,58]

$$\begin{aligned} A(x; p) * f_W^a(x; p) &= a f_W^a(x; p), \\ f_W^a(x; p) * A(x; p) &= a f_W^a(x; p), \end{aligned}$$ (35)

known as a $*$-genvalue problem (and it is possible to generalize this result to the case of degenerate spectrum [58]). Eq. (35) is a $*$-genvalue problem and represents in the Moyal formalism what the time-independent equation (1) represents in the Schrödinger formalism, when $A(x; p) = H(x; p) = M_W(\hat{H})$ (with $\hat{H}$ defined in (2)).

The time-dependent equation. In the very same way, it is possible to obtain the time-dependent evolution equation for the Wigner function $f_W(x; p; t)$. Indeed, supposing that the wave-functions $\psi(x; t)$ is a solution of the Schrödinger equation (3), one can show that the function f_W obeys to the following evolution equation:

$$\frac{\partial f_W(x; p; t)}{\partial t} = [H, f_W(x; p; t)]_M,$$ (36)

which corresponds the single-body Wigner equation in the Moyal formalism and it is equivalent to Eq. (10). In this formulation of quantum mechanics, this corresponds to the time-dependent Schrödinger equation (3).

2.5. Admissible states in phase-space

More recently, the work of Tatarskii [66] and Dias and Prata [58] have shown what the definition, conditions and properties for admissible pure and mixed states are in the phase-space formulation of quantum mechanics [58]. This is twofold. On the one hand, it helps us to define what properties a phase-space function (a $c-$number) must have in order to be a valid description of a state in the Wigner formalism (in other words, not every function defined over the phase-space is a valid physical description). On the other hand, it shows that the Wigner formalism can be defined in a completely independent form from the Schrödinger formulation.

Definition of quantum pure states. A distribution function $f_W(x; p)$ is said to represent a *pure quantum state* in the Wigner formalism if it can be expressed in terms of only one pure state wave-function. Formula (4) is an example of pure state. Pure quantum states correspond to valid descriptions of physical systems. Thus, an important question that raises from these definitions is, given a real valued and normalized function defined over the phase-space $f = f(x; p)$, how to determine if it is a pure state. In the following we report mathematical properties that *all* phase-space functions must satisfy to be valid representations of a pure state in the Wigner formalism. In order to answer to this question we make use of the results presented in [58].

Condition 1. Given a real valued, normalized function $f = f(x; p)$ defined over the phase-space, one can show that it represents a pure state *if and only if* it satisfies the following condition:

$$f * f = \frac{1}{2\pi\hbar} f.$$ (37)

Thus, given a function defined by (4) with ψ a normalized complex valued function, it satisfies condition (37). Conversely, given a normalized real valued function fulfilling property (37), it is a valid pure state in the Wigner formalism. While this is a very elegant and concise way to check whether a phase-space function represents a pure state, in practice it may be difficult to evaluate the $*$-product involved in (37). A more practical way is provided by the following condition.

Condition 2. Let $f = f(x; p)$ be a square integrable phase-space function and

$$Z(x; j) = \int dp e^{ijp} f(x; p),$$

a function of the position x and variable j. The function $f(x; p)$ can be expressed in the form:

$$f(x; p) = \frac{1}{(\hbar \pi)} \int_{-\infty}^{+\infty} dx' \, \psi_a^*(x + x') \psi_b(x - x') e^{-\frac{2i}{\hbar} x' \cdot p},$$

with $\psi_a(x)$ and $\psi_b(x)$ two complex square integrable functions, if the function $Z(x; j)$ satisfies the following (non-linear) partial differential equation:

$$\frac{\partial^2}{\partial j^2} \ln Z(x; j) = \left(\frac{\hbar}{2} \right)^2 \frac{\partial^2}{\partial x^2} \ln Z(x; j). \tag{38}$$

Moreover, if the function $f(x; p)$ is real and normalized then it represents a pure quantum state in the Wigner formalism. Conversely, if the function $f(x; p)$ is a pure state then it satisfies (38). An alternative (but equivalent) way to check if a phase-space function represents a pure state is obtained by introducing the following function:

$$\Sigma(y; p) = \int dx e^{ixy} f(x; p).$$

It can be shown that a normalized real valued function $f(x; p)$ is a quantum pure state if and only if

$$\frac{\partial^2}{\partial y^2} \ln \Sigma(y; p) = \left(\frac{\hbar}{2} \right)^2 \frac{\partial^2}{\partial p^2} \ln \Sigma(y; p). \tag{39}$$

Eq. (39) represents an alternative way to the condition (38) which might be easier to evaluate depending on the specific case.

We call Eq. (38) the *pure state quantum condition* which was introduced in 1983 by V. Tatarskii [66]. In the following, we report several properties for pure quantum states valid in the phase-space formulation of quantum mechanics. While we do not make any direct use of these results here, it is important to report them since they allow a direct connection to the Schrödinger formalism. Indeed they provide a way to calculate the corresponding wave-functions of a given phase-space function. Moreover, these theorems provide conditions which must be fulfilled by a phase-space function to be a proper Wigner quasi-distribution describing a physical system.

Theorem 1. *Let the time-dependent function $f = f(x; p; t)$ satisfies the pure state quantum condition (38) at initial time $t = 0$, and let its time evolution be governed by the Moyal equation (36). Then the function $f(x; p; t)$ satisfies the pure state quantum condition for every t.*

Theorem 2. *Given a generic and linear operator $\hat{A}$ and a corresponding phase-space function $A = A(x; p)$ defined as*

$$A(x; p) = M_W \left(\hat{A} \right),$$

then the solution of the following $*$-genvalue problem

$$\begin{aligned} A(x; p) * f(x; p) &= a f(x; p), \\ f(x; p) * A(x; p) &= b f(x; p), \end{aligned} \tag{40}$$

with a and b belonging to the spectrum of $\hat{A}$, is a pure state and its corresponding wave-functions satisfy the eigenvalue problems

$$\begin{aligned} \hat{A} \psi_a(x) &= a \psi_a(x), \\ \hat{A}^\dagger \psi_b(x) &= b^* \psi_b(x), \end{aligned}$$

with $\hat{A}^\dagger$ the adjoint of $\hat{A}$.

Theorem 3. *If a function $f_W(x; p)$ satisfies the $*$-genvalue problem (35), then the associated wave-function ψ is given by*

$$\psi(x) = N \int dp e^{i \frac{px}{\hbar}} f_W \left(\frac{x}{2}; p \right) = N Z \left(\frac{x}{2}; \frac{x}{\hbar} \right), \tag{41}$$

where N is a normalization constant. The function $\psi(x)$ satisfies the eigenproblem (1).

In particular, these theorems prove that the solutions of the general $*$-genvalue problem (40) are pure states associated to the wave-functions satisfying the corresponding eigenvalue problem and are given by (41). These results provide a complete generalization and specification for pure states in the Wigner formalism.

Finally, it is important to note that the pure state quantum condition (38) implies the Heisenberg principle of uncertainty [58]. Following the example of Tatarskii [58,66] let us consider a Hamiltonian quadratic in position and momentum. In the specific case of a simple harmonic oscillator, the Hamiltonian of the system reads

$$H(x; p) = \frac{p^2}{2m} + \frac{1}{2}m\omega^2 x^2,$$

and the Moyal equation (36) reduces to the (classical) Liouville equation [58]

$$[H(x; p), f_W(x; p)]_M = -\frac{p}{m}\frac{\partial f_W}{\partial x} + m\omega^2 x \frac{\partial f_W}{\partial p} = 0. \tag{42}$$

It is possible to show that, in this case, any function of the Hamiltonian $H(x; p)$ is a solution of (42). In particular we construct the following solution

$$f_W(x; p) = \frac{a\omega}{2\pi}e^{-aH(x;p)} \tag{43}$$

(with a a positive real constant) which is real, normalized and square integrable. The position and momentum dispersions read

$$(\sigma_x)^2 = \langle \hat{x}^2 \rangle - \langle \hat{x} \rangle^2 = \frac{1}{ma\omega^2},$$

$$(\sigma_p)^2 = \langle \hat{p}^2 \rangle - \langle \hat{p} \rangle^2 = \frac{m}{a}.$$

Thus

$$\sigma_x \cdot \sigma_p = \frac{1}{a\omega},$$

which has no lower bound since a is an arbitrary constant, in disagreement with the uncertainty principle of Heisenberg. This means that the proposed solution is not an acceptable quantum state in the Wigner formalism. This is an important point. As a matter of fact, this example shows in a clear manner that not every phase-space function is an acceptable state in the Wigner formalism. The pure state condition (38) must be fulfilled. If we, now, impose this condition to f_W one obtains:

$$a = \frac{2}{\hbar\omega},$$

which now introduces the following relation

$$\sigma_x \cdot \sigma_p = \frac{\hbar}{2},$$

i.e. a even more restrictive condition than the uncertainty principle of Heisenberg [58,66].

2.6. Interpretation of negative probabilities

The Wigner quasi-distribution function defined in (4), (16) for single-body problem (in pure and mixed state respectively), and in (21), (22) for the many-body problem (in pure and mixed states respectively), retains many of the properties of a classical distribution function. As a matter of fact, one can use it to compute the average value of a macroscopic variable. The only difference consists in the negative values the Wigner function can have in some region of the phase-space. In this section, we suggest a reasonable interpretation of these *negative probabilities* based on the experimental evidences presented in [43,44], and [45] in the context of quantum tomography. To this aim, we start by discussing the convolution of the Wigner function. Then we briefly sketch how the Wigner function of an experiment setting is reconstructed. From the previous two points we suggest an interpretation of the (sometimes occurring) negative values.

Convolution of the Wigner function. In order to compute the average value of a macroscopic variable $A = A(\mathbf{x}; \mathbf{p})$, one utilizes formula (5) which is essentially a convolution of the Wigner function. This creates a direct connection to classical (statistical) mechanics. In the convolution process, the Wigner function $f_W = f_W(\mathbf{x}; \mathbf{p}; t)$ is multiplied by a function $A(\mathbf{x}; \mathbf{p})$ which can be naturally interpreted as the phase-space probability of possible states of a measurement device (distributed over an area of order $\hbar$ or larger) [44,45]. In particular, when the resolution of the measuring device is degraded away, such that the Heisenberg uncertainty principle do not play any important role any longer, localized regions of $f_W(\mathbf{x}; \mathbf{p}; t)$ (which may contain negative values) are washed out and formula (5) becomes completely classical [45].

Quantum tomography. We have seen that the probability distribution of any physical observable corresponds to an integration of the Wigner function. Therefore, it seems that any measurement cannot provide localized values of the
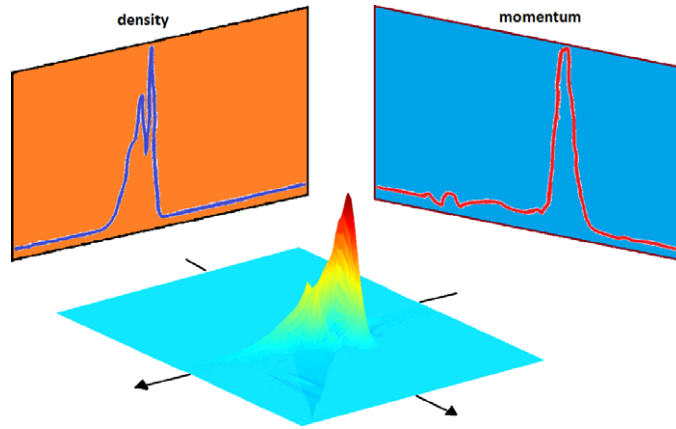
Fig. 1. Artistic representation of a Wigner quasi-distribution function along with its projections (integral) over space and momentum.

$f_W(\mathbf{x}; \mathbf{p}; t)$. Despite these difficulties, an experimental technique known as quantum tomography has been developed which can reconstruct the Wigner function of an experimental setting [44,45]. Essentially, the technique relies on the fact that an experiment can be prepared and repeated a large amount of times, thus providing a projection of the Wigner function. For example, one may first measure the position of a particle for a large enough number of times and then repeat the same experiment measuring the momentum of the particle. In practice, this provides a projection of the Wigner function over the position and momentum directions of the phase-space frame. Then, it is possible to apply an inverse Radon transformation which reconstruct the (higher dimensional) function f_W [44,45], along with its (eventual) negative values (see Fig. 1).

An interpretation of the negative values in f_W can now be provided. The Wigner quasi-distribution function is the quantum mathematical object which most closely corresponds to a classical distribution function. It is utilized to compute the average value of macroscopic variables but it is not a proper distribution function as it may have localized negative values. Now, classical particles are always localized in a precise point of the phase-space, and a ensemble of classical particles can define a proper distribution function. But when dealing with quantum particles, the Heisenberg principle of uncertainty prevents such localization, forcing the description of a particle to an area of the phase-space bigger $\Delta x \Delta p = \frac{\hbar}{2}$. In other words, this means that if the position is well known, i.e. highly localized, then the momentum is delocalized and vice versa. This feature has to be included in a proper description of the quantum world and is clearly exhibited by the appearance of negative values in the Wigner function. Therefore, one may infer that areas of the phase-space with a negative sign are essentially regions which are experimentally forbidden by the uncertainty principle [45].

3. The Wigner Monte Carlo method for single-body systems

The Monte Carlo theory to solve the single-body Wigner equation represents an important achievement in the field of simulations of quantum systems composed of one particle only. In this section, we focus on the signed particle Monte Carlo (MC) method [53,54,67] and a particular attention to details is given in order to put the reader in the conditions to duplicate the method and the results. This method has been recently validated against well-known numerical tests.

This is an important section of this paper. All details provided here need attention to be understood. The next two sections, and the applications shown at the end of this paper, depend on this section. They cannot be understood without a comprehension of this section. Therefore, we strongly recommend the reader to carefully go through the mathematical details. Furthermore, an implementation of the Wigner MC method described here is available at [68]. The reader is advised to download the source code and study it for a complete understanding.

3.1. Semi-discrete phase-space

We recall that in the Wigner formulation of quantum mechanics [11] a quantum system consisting of one particle is completely described in terms of a phase-space quasi-distribution function $f_W(\mathbf{x}; \mathbf{p}; t)$ evolving according to Eq. (10). Thus, our aim is to reconstruct the function f_W at a given time. We start by reformulating the Wigner equation in a semi-discrete phase-space with a continuous spatial variable $\mathbf{x}$ and a discretized momentum $\mathbf{p}$ described in terms of a step $\Delta \mathbf{p} = \frac{\hbar \pi}{L_C}$, where L_C is a free parameter defining the discretization (and a study on the dependence of the quality of a solution in function of L_C has been carried out in [69]). Now, the semi-discrete Wigner equation reads:

$$\frac{\partial f_W}{\partial t} + \frac{\hbar}{m} \frac{\mathbf{M} \Delta \mathbf{p}}{\hbar} \cdot \nabla_{\mathbf{x}} f_W = \sum_{M'=-\infty}^{+\infty} V_W(\mathbf{x}; \mathbf{M}'; t) f_W(\mathbf{x}; \mathbf{M} - \mathbf{M}'; t), \tag{44}$$

where, for convenience, we use the notation $f_W(\mathbf{x}; \mathbf{M}; t) = f_W(\mathbf{x}; \mathbf{M}\Delta\mathbf{p}; t)$, with $\mathbf{M} = (M_1, \ldots, M_d)$ a set of integers with d elements, and $\mathbf{M}\Delta\mathbf{p} = (M_1\Delta p_1, \ldots, M_d\Delta p_d)$. In particular, once one knows the Wigner function of a system, it is useful to evaluate the expectation value $\langle A \rangle(t)$ of some generic physical quantity, described by a phase-space function, or c-number, $A = A(x; k)$ at a given time t. Thus, our computational problem reduces to the calculation of the inner product (A, f_W) with the solution of (10). It can be shown that this task can be reformulated in a way which involves the solution of the adjoint equation. Doing this, we first obtain an integral form of (10), and then the adjoint equation.

3.2. Integral formulation

The semi-discrete Wigner equation (44) can be reformulated in a integral form. First, one defines a function γ as

$$\gamma(\mathbf{x}) = \sum_{\mathbf{M}=-\infty}^{\infty} V_w^+(\mathbf{x}; \mathbf{M}) = \sum_{\mathbf{M}=-\infty}^{\infty} V_w^-(\mathbf{x}; \mathbf{M}), \tag{45}$$

where V_w^+ is the positive part of V_w, i.e. it gives V_W if $V_w > 0$ and 0 otherwise, and V_w^- is the negative part defined similarly (the equality was first proven in [67], then in [53] and, again, in [54]). Let us, now, add and subtract the term $\gamma(\mathbf{x}(t'))$ to Eq. (44). Furthermore, let us introduce the following quantity:

$$\Gamma(\mathbf{x}(t'), \mathbf{M}, \mathbf{M}') = V_w^+(\mathbf{x}(t'); \mathbf{M} - \mathbf{M}') - V_w^+(\mathbf{x}(t'); -(\mathbf{M} - \mathbf{M}')) + \gamma(\mathbf{x}(t'))\delta_{\mathbf{M},\mathbf{M}'}. \tag{46}$$

By integrating over the interval $(0, t)$, supposing that initial conditions are imposed at time 0, one can include both boundary and initial conditions in the formulation and obtain the following equation:

$$\begin{aligned}
&f_W(\mathbf{x}; \mathbf{M}; t) - e^{-\int_0^t \gamma(\mathbf{x}(y))dy} f_i(\mathbf{x}(0); \mathbf{M}) \\
&= \int_0^t dt' \sum_{\mathbf{M}'=-\infty}^{\infty} f_W(\mathbf{x}(t'); \mathbf{M}'; t') \Gamma(\mathbf{x}(t'), \mathbf{M}, \mathbf{M}') e^{-\int_{t'}^t \gamma(\mathbf{x}(y))dy} \\
&= \int_0^\infty dt' \sum_{\mathbf{M}'}^{\infty} \int dx' f_W(\mathbf{x}'; \mathbf{M}'; t') \Gamma(\mathbf{x}', \mathbf{M}, \mathbf{M}') e^{-\int_{t'}^t \gamma(\mathbf{x}(y))dy} \theta(t - t')\delta(\mathbf{x}' - \mathbf{x}(t'))\theta_D(\mathbf{x}'),
\end{aligned} \tag{47}$$

where, to ensure the explicit appearance of the variables $Q = (\mathbf{x}, \mathbf{M}, t)$ and $Q' = (\mathbf{x}', \mathbf{M}', t')$, the kernel has been augmented by the θ and δ functions which retain the value of the integral unchanged. In particular θ_D keeps the integration within the simulation domain (if any). In the same way, the expectation value of the physical quantity A at time τ is augmented and reads:

$$\langle A \rangle(\tau) = \int dt \int d\mathbf{x} \sum_{\mathbf{M}=-\infty}^{\infty} f_W(\mathbf{x}; \mathbf{M}; t)A(\mathbf{x}; \mathbf{M})\delta(t - \tau) = \int dQ f_W(Q)A_\tau(Q), \tag{48}$$

(note the implicit definition of the symbol $A_\tau(Q)$).

3.3. Adjoint equation

One can rewrite the expectation value (48) by formally introducing the adjoint equation of (47) which has a solution g and a free term g_0 determined below:

$$f(Q) = \int dQ' K(Q, Q')f(Q') + f_i(Q), \qquad g(Q') = \int dQ K(Q, Q')g(Q) + g_0(Q').$$

We now multiply the first equation by $g(Q)$, and integrate over Q. Then, we multiply the second equation by $f(Q')$ and integrate over Q'. Finally, we subtract the two equations. One obtains:

$$\int dQ f_i(Q)g(Q) = \int dQ' g_0(Q')f(Q')$$

$$\int dQ' f_i(Q')g(Q') = \int dQ g_0(Q)f(Q),$$

where the dummy variables have been exchanged for a more convenient comparison with (48). In particular, this shows that:

$$g_0(Q) = A_\tau(Q);$$

$$\langle A \rangle = \int_0^\infty dt' \int d\mathbf{x}' \sum_{\mathbf{M}'=-\infty}^{\infty} f_i(\mathbf{x}'; \mathbf{M}')e^{-\int_0^{t'} \gamma(\mathbf{x}'(y))dy} g(\mathbf{x}'; \mathbf{M}'; t'), \tag{49}$$

where $\mathbf{x}'(y)$ is the trajectory initialized by $(\mathbf{x}', \mathbf{M}', t')$, and $\mathbf{x}(0) = \mathbf{x}'$. Thus, one obtains the adjoint equation by integration on the unprimed variables:

$$g(\mathbf{x}'; \mathbf{M}'; t') = A_\tau(\mathbf{x}', \mathbf{M}', t')$$
$$+ \int_0^\infty dt \sum_{\mathbf{M}=-\infty}^{\infty} \int d\mathbf{x}\, g(\mathbf{x}; \mathbf{M}; t) \Gamma(\mathbf{x}', \mathbf{M}, \mathbf{M}') e^{-\int_{t'}^{t} \gamma(\mathbf{x}(y))dy} \theta(t - t') \delta(\mathbf{x}' - \mathbf{x}(t')) \theta_D(\mathbf{x}'). \tag{50}$$

This equation is further modified by reverting the parametrization of the field-less trajectory. Now $(\mathbf{x}(t') = \mathbf{x}'', \mathbf{M}, t')$ initialize the trajectory and the variable $\mathbf{x} = \mathbf{x}(t)$ becomes the time dependent variable. Finally, the spatial coordinates for the function g becomes $\mathbf{x}'(t)$. Thus one obtains:

$$g(\mathbf{x}'; \mathbf{M}'; t') = A_\tau(\mathbf{x}', \mathbf{M}', t') + \int_{t'}^\infty dt \sum_{\mathbf{M}=-\infty}^{\infty} g(\mathbf{x}'(t); \mathbf{M}; t) \Gamma(\mathbf{x}', \mathbf{M}, \mathbf{M}') e^{-\int_{t'}^{t} \gamma(\mathbf{x}'(y))dy} \theta_D(\mathbf{x}'). \tag{51}$$

In the same way, by reverting the parametrization of the field-less trajectory, Eq. (49) is reformulated, with the initialization changing from $(\mathbf{x}', \mathbf{M}', t')$ to $(\mathbf{x}_i = \mathbf{x}'(0), \mathbf{M}', 0)$:

$$\mathbf{x}'(y) = \mathbf{x}_i(y) = \mathbf{x}_i + \frac{\mathbf{M}' \Delta \mathbf{p}}{m} y; \qquad \mathbf{x}' = \mathbf{x}'(t') = \mathbf{x}_i(t'); \qquad d\mathbf{x}' = d\mathbf{x}_i$$

$$\langle A \rangle = \int_0^\infty dt' \int d\mathbf{x}_i \sum_{\mathbf{M}'=-\infty}^{\infty} f_i(\mathbf{x}_i; \mathbf{M}') e^{-\int_0^{t'} \gamma(\mathbf{x}_i(y))dy} g(\mathbf{x}_i(t'); \mathbf{M}'; t'). \tag{52}$$

3.4. Signed particle method

By consecutive iterations of (50) into (52) it is now possible to depict a numerical method based on particles. The zero-th order term reads:

$$\langle A \rangle_0(\tau) = \int_0^\infty dt' \int d\mathbf{x}_i \sum_{\mathbf{M}'=-\infty}^{\infty} f_i(\mathbf{x}_i; \mathbf{M}') e^{-\int_0^{t'} \gamma(\mathbf{x}_i(y))dy} A(\mathbf{x}_i(t'); \mathbf{M}') \delta(t' - \tau).$$

By applying the Monte Carlo theory for the computation of integrals, one can interpret part of the integrand as a product of conditional probabilities in the following way. Assuming that f_i is normalized to unity, one generates a set of random points $(\mathbf{x}_i, \mathbf{M}')$ at time 0 which initialize the particle trajectories $\mathbf{x}_i(y)$. Thus, the exponent gives the probability for a particle to remain over the trajectory provided that the *change-of-trajectory* rate is represented by the function γ. In practice, this probability filters out these particles, such that the randomly generated *change-of-trajectory* time is less than τ. If a particle stays in the trajectory until time τ, then it contributes to $\langle A \rangle_0(\tau)$ with a value equal to the rest of the integrand, i.e. $f_i(\mathbf{x}_i; \mathbf{M}') A(\mathbf{x}_i(\tau), \mathbf{M}')$. Otherwise, particles which have experienced a change-of-trajectory event do not contribute at all. Finally, $\langle A \rangle_0(\tau)$ is estimated by averaging over the set of N initialized particles.

Similarly, the first order term of the iteration term is obtained by replacing the term $g(\mathbf{x}_i(t'); \mathbf{M}'; t')$ in (52) by the kernel of (51) specifically rewritten (in other words in (51) we substitute $\mathbf{x}'$ with $\mathbf{x}_1 = \mathbf{x}_i(t')$). Note that the trajectory in the exponent is now initialized by the values $(\mathbf{x}_1, \mathbf{M}, t')$:

$$\langle A \rangle_1(\tau) = \int_0^\infty dt' \int d\mathbf{x}_i \sum_{\mathbf{M}'=-\infty}^{\infty} f_i(\mathbf{x}_i; \mathbf{M}') e^{-\int_0^{t'} \gamma(\mathbf{x}_i(y))dy}$$
$$\times \int_{t'}^\infty dt \sum_{\mathbf{M}=-\infty}^{\infty} g(\mathbf{x}_1(t); \mathbf{M}; t) \Gamma(\mathbf{x}_1, \mathbf{M}, \mathbf{M}') e^{-\int_{t'}^{t} \gamma(\mathbf{x}_1(y))dy} \theta_D(\mathbf{x}_1).$$

Then, we replace the function $g(\mathbf{x}_1(t); \mathbf{M}; t)$ with the free term of Eq. (51) at point $A(\mathbf{x}_1(t), \mathbf{M}, t) \delta(t - \tau)$. Finally, we augment the equation by completing some of the probabilities enclosed in curly brackets and we partially reorder some of the terms to obtain:

$$\langle A \rangle_1(\tau) = \int_0^\infty dt' \int d\mathbf{x}_i \sum_{\mathbf{M}'=-\infty}^{\infty} f_i(\mathbf{x}_i; \mathbf{M}') \left\{ \gamma(\mathbf{x}_i(t')) e^{-\int_0^{t'} \gamma(\mathbf{x}_i(y))dy} \right\}$$
$$\times \theta_D(\mathbf{x}_1) \int_{t'}^\infty dt \sum_{\mathbf{M}=-\infty}^{\infty} \left\{ \frac{\Gamma(\mathbf{x}_1, \mathbf{M}, \mathbf{M}')}{\gamma(\mathbf{x}_i(t'))} \right\} \left\{ e^{-\int_{t'}^{t} \gamma(\mathbf{x}_1(y))dy} \right\} A(\mathbf{x}_1(t), \mathbf{M}, t) \delta(t - \tau).$$

One can give a similar Monte Carlo interpretation. A particle is now initialized at $(\mathbf{x}_i, \mathbf{M}', 0)$. It follows the trajectory until time t', i.e. the time the particle leaves the initial trajectory (or equivalently changes its coordinates in the phase-space).

The time t' is given by the probability density in the first curly brackets. Indeed, the enclosed term, if integrated over the time interval $(0, \infty)$, gives unity. Furthermore, the exponent represents the probability for a particle of staying in the same trajectory until time t', while $\gamma(\mathbf{x}_i(t'))dt'$ is the probability to leave that trajectory in the interval $(t', t' + dt')$. The phase-space position now becomes $\left(\mathbf{x}_1 = \mathbf{x}_i(t'), \mathbf{M}'\right)$ at t' and the evolution continues (if the particle is still in the simulation domain, otherwise its contribution is zero). The term in the next curly bracket is interpreted as a source of momentum change from $\mathbf{M}'$ to $\mathbf{M}$ (locally in space at point $\mathbf{x}_1$ and at the time of scattering t'). Thus, at moment t' the particle initializes the trajectory $(\mathbf{x}_1, \mathbf{M})$ and, with the probability given by the exponent in the last curly brackets, remains over the trajectory until time τ. In particular, t is set to τ by the δ function provided that $t' < \tau$, otherwise the contribution is zero. We note however that in this case the particle has a contribution to the zero-th iteration term.

In the very same way, one can calculate the first three terms and sum them up to show how to continue with higher order terms:

$$
\sum_{s=0}^{2} \langle A \rangle_s(\tau) = \int_0^\tau dt_i \int d\mathbf{x}_i \sum_{\mathbf{M}_i = -\infty}^{\infty} f_i(\mathbf{x}_i; \mathbf{M}_i) \, e^{-\int_0^{t_i} \gamma(\mathbf{x}_i(y))dy}_{\Uparrow \mathbf{x}_i, \mathbf{M}_i, 0}
$$

$$
\times \left[A(\mathbf{x}_1, \mathbf{M}_i) \, \delta(t_i - \tau) + \int_{t_i}^\tau dt_1 \sum_{\mathbf{M}_1 = -\infty}^{\infty} \theta_D(\mathbf{x}_1) \, \Gamma(\mathbf{x}_1, \mathbf{M}_1, \mathbf{M}_i) \, e^{-\int_{t_i}^{t_1} \gamma(\mathbf{x}_1(y))dy}_{\Uparrow \mathbf{x}_1, \mathbf{M}_1, t_i} \right.
$$
$$
{}_{\Uparrow \mathbf{x}_1 = \mathbf{x}_i(t_i)}
$$

$$
\times \left[A(\mathbf{x}_2, \mathbf{M}_1) \, \delta(t_1 - \tau) + \int_{t_1}^\tau dt_2 \sum_{\mathbf{M}_2 = -\infty}^{\infty} \theta_D(\mathbf{x}_2) \, \Gamma(\mathbf{x}_2, \mathbf{M}_2, \mathbf{M}_1) \, e^{-\int_{t_1}^{t_2} \gamma(\mathbf{x}_2(y))dy}_{\Uparrow \mathbf{x}_2, \mathbf{M}_2, t_1} \, A(\mathbf{x}_3, \mathbf{M}_2) \, \delta(t_2 - \tau)_{\Uparrow \mathbf{x}_3 = \mathbf{x}_2(t_2)} \right] \right] .
$$
$$
{}_{\Uparrow \mathbf{x}_2 = \mathbf{x}_1(t_1)}
$$

The initialization coordinates of the novel trajectories are denoted by the symbol $\Uparrow$.

It is clear that the iteration expansion of $\langle A \rangle$ branches, and the total value is given by the sum of all branches. Thus instead of changing trajectory, one may interpret the sum as three new trajectory pieces or, equivalently, three *signed* particles appearing:

$$
\frac{\Gamma(\mathbf{x}_1, \mathbf{M}, \mathbf{M}')}{\gamma(\mathbf{x}_1)} = \left\{ \frac{V_w^+(\mathbf{x}_1, \mathbf{M} - \mathbf{M}')}{\gamma(\mathbf{x}_1)} \right\} - \left\{ \frac{V_w^-(\mathbf{x}_1, \mathbf{M} - \mathbf{M}')}{\gamma(\mathbf{x}_1)} \right\} + \left\{ \delta_{\mathbf{M}, \mathbf{M}'} \right\} . \tag{53}
$$

A short analysis of the last term suggests that the initial (parent) particle survives and two more particles (one positive and one negative) are generated with the first two probabilities (in curly brackets). Equivalently, one generates the first state $\mathbf{M} - \mathbf{M}' = \mathbf{L}$ with probability

$$
\frac{V_w^+(\mathbf{x}_1, \mathbf{L})}{\gamma(\mathbf{x}_1)} .
$$

Thus, using the same probability, or simply a new random number, one generates another value, say $\mathbf{L}'$, and obtains a second state $\mathbf{M}' - \mathbf{M} = \mathbf{L}'$. It is easy to see that, actually, these values can be combined into a single choice of $\mathbf{L}$ by reordering the sum over $\mathbf{M}$ for the second term so that $V_w^-(\mathbf{x}_1, \mathbf{M} - \mathbf{M}')$ appears in the place of V_w^+. Indeed, we recall that if $V_w^+(\mathbf{L})$ is not zero then $V_w^+(-\mathbf{L}) = 0$ and $V_w^-(-\mathbf{L}) = V_w^+(\mathbf{L})$. In this way the following two states, with the second one having a flipped sign, have the same probability to appear:

$$
\mathbf{M} - \mathbf{M}' = \mathbf{L}, \qquad \mathbf{M} - \mathbf{M}' = -\mathbf{L};
$$

or equivalently

$$
\mathbf{M} = \mathbf{M}' + \mathbf{L}, \qquad \mathbf{M} = \mathbf{M}' - \mathbf{L}.
$$

We can now summarize the outcomes obtained so far. By applying the kernel of (51) in the form (53), one can order the terms of the resolvent expansion of (52). This is utilized to construct a transition probability for the numerical Monte Carlo trajectories which consist of pieces of Newton trajectories linked by a change of the momentum from $\mathbf{M}$ to $\mathbf{M}'$ according to Γ. These trajectories are interpreted as moving particles under events which change their phase-space coordinates. The exponent in the formulas gives the probability that a particle remains on its field-less Newton trajectory with a changing rate equal to γ. If the particle does not change trajectory until time τ, particles contribute to $\langle A \rangle_0(\tau)$ with the value $f_i(\mathbf{x}_i; \mathbf{M}')g(\mathbf{x}_i(\tau); \mathbf{M}')$, otherwise they contribute to a next term of the expansion. It can be proved that a particle contributes to one and only one term of this expansion. Thus, the macroscopic value $\langle A \rangle(t)$ is estimated by averaging over N particles.

Therefore, by exploiting the appearance of the term Γ, it is possible to depict a Monte Carlo algorithm for the ballistic, single-body, semi-discrete Wigner equation (44). After any free flight the initial particle creates two new particles with opposite signs and momentum offset (around the initial momentum) equal to $+\mathbf{L}$ and $-\mathbf{L}$ where $\mathbf{L} = \mathbf{M} - \mathbf{M}'$. The initial particle and the two newly created represent three contributive terms of the series. We, thus, have a Monte Carlo algorithm for our model.

3.5. The annihilation technique

It can be demonstrated that the process of creation of new couples is exponential [67]. By noting that, in the above depicted Monte Carlo method, particles are indistinguishable and annihilate when they belong to the same phase-space cell and have opposite signs, it is possible to remove a significant number of particles during the simulation. The technique has been largely documented in [70] and we only sketch the main tenets here. If one fixes a *recording* time step at which we check if particles belong to the same region of the phase-space with negative signs, then they are removed and all non-annihilating particles are kept in the simulation. These observations highlight the possibility of removing, periodically, all particles not contributing to the calculation of the Wigner function or, in other words, one can apply a renormalization of the numerical average of the Wigner quasi-distribution by means of a particles annihilation process. This is in accordance to the Markovian character of the evolution to progress at consecutive time steps so that the final solution at a given time step becomes the initial condition for the next step.

This technique has proved to be very efficient, especially for the simulation of realistic objects which typically involve several tens or even hundreds of millions of initial particles. Without this technique, time-dependent Monte Carlo simulations of the Wigner equation would be practically impossible *tout court*.

4. Extension to density functional theory

The simulation of quantum many-body systems is a complex task which is well-known to require immense computational resources. It is also an important problem which touches many aspects of our everyday life. For example, they allow the comprehension, and thus the design and exploitation, of complex chemical reactions, new materials, new electronics, etc. Therefore it is not surprising that a very early interest has been shown in this direction. In 1926 a first attempt to simplify the quantum many-body problem, although in the stationary case, was done by introducing an approximate method to find the electronic structure in terms of a one-electron ground-state density $\rho(\mathbf{x})$, [71,72]. The Thomas–Fermi theory, as it is known today, introduces too many oversimplifications to be of any practical use but it represents a foundational result for the development of DFT. Later on, Slater combined the ideas of Thomas and Fermi with the Hartree's orbital method [73,74], introducing for the first time a local exchange potential. Then the Hohenberg–Kohn theorem proved that, in principle, an exact method using the one-electron ground-state density $\rho(\mathbf{x})$ [75] can be depicted and the Kohn–Sham system was introduced from the homogeneous quantum electron gas theory [76]. The time-dependent counterpart of the Hohenberg–Kohn theorem was introduced in 1984 which is known as the Runge–Gross theorem [77]. One should note that this theorem guarantees the validity of the time-dependent Kohn–Sham system only for the calculations of the ground-state properties. Nothing is proved about the excited states. Finally, it is also known that the mapping from a given time-dependent potential to time-dependent density is not invertible and a time-dependent current-density functional theory is required [78].

Nowadays, the density functional theory (DFT) can be considered the most popular and utilized tool [79]. In this section we introduce an extension of the Wigner MC method to DFT as a way to simulate many-body problems. This section is based on the work described in [37].

4.1. The Kohn–Sham density functional theory

DFT relies on our capability of calculating the wave-function of a single-electron Schrödinger equation. Essentially, the quantum many-body problem is reduced to a system of coupled single-electron equations, known as the Kohn–Sham system, and effects such as electron–electron interaction are described in terms of the so-called density functional. This is the essence of both time-independent and time-dependent approaches in DFT [76,77]. This simplification allows the simulation of many-body problems in acceptable computational times, but the price to pay for it is that the exact mathematical expression for the density functional is known only for simple cases and further approximations are introduced for more complex systems. Despite the difficulties, nowadays one can choose among a plethora of functionals, e.g. the local density approximation (LDA) [76], the generalized gradient approximation [80] and the B3LYP [81].

Now, the dynamics of quantum many-body systems is described by the many-body Schrödinger equation:

$$i\hbar\frac{\partial}{\partial t}\Psi = \hat{H}\Psi,\tag{54}$$

where the unknown is the (complex) wave-function $\Psi = \Psi(\mathbf{x}_1, \ldots, \mathbf{x}_n)$, and the Hamiltonian $\hat{H}$, accounts for the various forces involved in the problem (see formulas (20) and (27) for example). The resolution of (54) represents an incredible mathematical challenge even when approached by numerical techniques. It is worth to mention that attempts in this direction have been made (direct MC minimization techniques [82]) but, up to now, they only allow the calculation of the stationary ground state.

Despite its limitations, the time-dependent Kohn–Sham system greatly reduces the difficulties involved in (54) and allows practical and useful (but not yet chemical/quantitative) simulations of quantum many-body systems. Indeed, we now deal with a set of n single-body Schrödinger equations coupled to each other by means of an artificial density functional $v_{\text{eff}}(\mathbf{x})$ which is local [79]. One should note that the locality of this functional introduces severe restrictions to the time-dependent simulations of strongly correlated electron systems.

In practice, the time-dependent Kohn–Sham system consists of the following set of equations ($i = 1 \ldots n$)

$$ i\hbar \frac{\partial \Phi_i}{\partial t}(\mathbf{x}, t) = \left(-\frac{\hbar^2 \nabla^2}{2m_i} + U_{\text{eff}}(\mathbf{x}) \right) \Phi_i(\mathbf{x}, t) \tag{55} $$

from which the one-electron density can be calculated in the following way:

$$ \rho(\mathbf{x}) = \sum_i |\Phi_i(\mathbf{x})|^2, \tag{56} $$

where the sum is performed over the states below the Fermi energy. The many-body effects are included in the effective potential $U_{\text{eff}} = U_{\text{eff}}(\mathbf{x})$ which can be expressed in terms of an external potential (usually representing the potential due to the nuclei of a molecule), the Hartree potential and an exchange–correlation potential

$$ U_{\text{eff}}(\mathbf{x}) = U_{\text{ext}}(\mathbf{x}) + e^2 \int d\mathbf{x}' \frac{\rho(\mathbf{x}')}{|\mathbf{x} - \mathbf{x}'|} + U_{\text{xc}}[\rho](\mathbf{x}). \tag{57} $$

Finally, one should note that there is no unique way to express the density functional U_{xc}. Many choices are available (e.g. [76,80] and [81]). In any case, given a functional, it is possible to solve the set of Eq. (55) from which one obtains the one-electron density $\rho(\mathbf{x})$.

4.2. The Wigner density functional theory

By applying the Wigner–Weyl transform (31) to every Schrödinger equation of the set (55), with $U(\mathbf{x}) = U_{\text{eff}}(\mathbf{x})$, one obtains a new time-dependent Kohn–Sham system expressed in terms of the corresponding n Wigner equations, i.e.:

$$ \frac{\partial f_w^i}{\partial t} + \frac{\mathbf{p}}{m_i} \cdot \nabla_{\mathbf{x}} f_w^i = Q[f_w^i], \tag{58} $$

where the Wigner potential is expressed in terms of an effective potential

$$ V_w(\mathbf{x}, \mathbf{p}, t) = \frac{i}{(2\pi)^d \hbar^{d+1}} \int d\mathbf{x}' e^{-i\frac{\mathbf{p} \cdot \mathbf{x}'}{\hbar}} \left(U_{\text{eff}}\left(\mathbf{x} + \frac{\mathbf{x}'}{2}, t\right) - U_{\text{eff}}\left(\mathbf{x} - \frac{\mathbf{x}'}{2}, t\right) \right). \tag{59} $$

Given an adequate effective potential $U_{\text{eff}}(\mathbf{x})$ which, in turn, depends on the choice of the exchange–correlation functional, the quantum many-body problem now consists of solving the set of coupled equations (58). This system, of course, being based on the same assumptions, is affected by the same problems of standard DFT. The choice of the exchange–correlation potential is not unique and difficult to select, there is no guarantee that the excited states are correct, etc. This approach, if applied to any computational quantum problem, will essentially give the same answers given by the standard DFT. Nevertheless, two important advantages appear in this new model. First, the Wigner formalism is based on the concept of a quasi-distribution function and, as such, offers a much more intuitive representation of the simulated system. For example, one can discuss the system in terms of single-electron distribution functions and visualize the time-dependent energy distribution which can give profound insights about the dynamics involved. Second, the Wigner MC method, based on the Iterative MC method, is known to be highly scalable outperforming other numerical approaches (one can reach very deep levels of parallelization almost trivially) [50,55]. This opens the way towards simulations of very complex structures.

5. The Wigner Monte Carlo method for many-body systems

Traditionally ab-initio simulations, based on first principles of quantum mechanics, are known to be an incredibly difficult task to perform. As a matter of fact, they require an immense amount of computational power. Although their complexity, it is important to be able to simulate such systems, since they allow the simulation of so-called *strongly correlated* systems, which are relevant in both applied physics and chemistry. In this section, the Wigner MC method for the single-body equation is generalized to the quantum many-body problem without introducing any supplementary physical approximation.

5.1. Semi-discrete phase-space

As done previously for the single-body Wigner equation, one starts by reformulating the many-body Wigner equation (23) in a semi-discrete phase-space with continuous spatial coordinates $\mathbf{x}$ and discretized momenta $\mathbf{p}$ expressed as multiples of the quantity $\Delta\mathbf{p} = \frac{\hbar\pi}{L_C}$, where L_C is the usual parameter which specifies the momentum discretization.

The semi-discrete many-body Wigner equation reads:

$$ \frac{\partial f_W}{\partial t}(\mathbf{x}; \mathbf{M}; t) + \sum_{k=1}^{n} \frac{\mathbf{M}_k \Delta\mathbf{p}}{m_k} \cdot \nabla_{\mathbf{x}_k} f_W = \sum_{\mathbf{M}=-\infty}^{+\infty} f_W(\mathbf{x}; \mathbf{M}; t) V_W(\mathbf{x}; \mathbf{M}; t), \tag{60} $$

with $\mathbf{M} = (\mathbf{M}_1, \mathbf{M}_2, \ldots, \mathbf{M}_n)$, $\sum_{\mathbf{M}=-\infty}^{+\infty} = \sum_{\mathbf{M}_1=-\infty}^{+\infty} \sum_{\mathbf{M}_2=-\infty}^{+\infty} \cdots \sum_{\mathbf{M}_n=-\infty}^{+\infty}$, and

$$V_W(\mathbf{x}; \mathbf{M}; t) = \frac{i}{\pi^{dn} \hbar^{dn+1}} \int d\mathbf{x}' e^{-\left(\frac{2i}{\hbar}\right) \sum_{k=1}^{n} \mathbf{x}'_k \cdot \mathbf{M}_k \Delta \mathbf{p}} \left[V\left(\mathbf{x} + \frac{\mathbf{x}'}{2}; t\right) - V\left(\mathbf{x} + \frac{\mathbf{x}'}{2}; t\right) \right].$$

Note that, now, the momentum of the ith particle is expressed as a set of d integers $\mathbf{M}_i = (M_1^i, \ldots, M_d^i)$ and $\mathbf{M}_i \Delta \mathbf{p} = (M_1^i \Delta p_1, \ldots, M_d^i \Delta p_d)$ where $\Delta \mathbf{p} = (\Delta p_1, \ldots, \Delta p_d)$.

5.2. Integral formulation

Eq. (60) can be rewritten in an integral form. To this aim, we first define the function γ in a many-body context as:

$$\gamma(\mathbf{x}) = \sum_{\mathbf{M}=-\infty}^{\infty} V_W^+(\mathbf{x}; \mathbf{M}), \tag{61}$$

where V_W^+ is, again, the positive part of V_W. Then, Eq. (60) can be rewritten by adding and subtracting the term $\gamma(\mathbf{x})$.

In the same way, the quantity Γ can be generalized and has the following expression:

$$\Gamma(\mathbf{x}; \mathbf{M}; \mathbf{M}') = V_W^+(\mathbf{x}; \mathbf{M} - \mathbf{M}') - V_W^+(\mathbf{x}; -(\mathbf{M} - \mathbf{M}')) + \gamma(\mathbf{x})\delta_{\mathbf{M},\mathbf{M}'}. \tag{62}$$

As usual, we assume that the evolution of an initial condition $f_i(\mathbf{x}; \mathbf{M})$ starts at time 0 and, by following the same strategy employed in the single-body Wigner MC method, one can rewrite the semi-discrete many-body Wigner equation in the form of a Fredholm integral equation of second kind:

$$f_W(\mathbf{x}; \mathbf{M}; t) - e^{-\int_0^t \gamma(\mathbf{x}(y))dy} f_i(\mathbf{x}(0); \mathbf{M})$$

$$= \int_0^\infty dt' \sum_{\mathbf{M}'=-\infty}^{+\infty} \int d\mathbf{x}' f_W(\mathbf{x}'; \mathbf{M}'; t') \Gamma(\mathbf{x}'; \mathbf{M}; \mathbf{M}') e^{-\int_{t'}^t \gamma(\mathbf{x}(y))dy} \theta(t - t') \delta(\mathbf{x}' - \mathbf{x}(t')) \theta_D(\mathbf{x}'). \tag{63}$$

One note that, in order to ensure the explicit appearance of the variables $\mathbf{Q} = (\mathbf{x}; \mathbf{M}; t)$ and $\mathbf{Q}' = (\mathbf{x}'; \mathbf{M}'; t')$, the kernel has been augmented by the θ and δ functions. Following the generalization of the signed particle MC method, one expresses the many-body expectation value of the physical quantity $A = A(\mathbf{Q})$ at time τ as:

$$\langle A \rangle(\tau) = \int dt \int d\mathbf{x} \sum_{\mathbf{M}=-\infty}^{\infty} f_W(\mathbf{x}; \mathbf{M}; t) A(\mathbf{x}; \mathbf{M}) \delta(t - \tau) = \int d\mathbf{Q} f_W(\mathbf{Q}) A_\tau(\mathbf{Q}). \tag{64}$$

5.3. Signed particle method

Formally speaking, one quickly realize that the equations so far recovered are in the same shape as the ones of the single-particle Wigner MC method. This suggests that one can simply follow the same procedure and express the expectation value (64) as a Liouville–Neumann series which help depicting a signed particle MC method for the many-body Wigner equation.

Thus, it is straightforward to obtain the zero-th order term of the series which reads:

$$\langle A \rangle_0(\tau) = \int_0^\infty dt' \int d\mathbf{x} \sum_{\mathbf{M}'=-\infty}^{\infty} f_i(\mathbf{x}; \mathbf{M}') e^{-\int_0^{t'} \gamma(\mathbf{x}(y))dy} A(\mathbf{x}(t'), \mathbf{M}') \delta(t' - \tau).$$

As usual, the mathematical Monte Carlo theory for solving integrals suggests to consider part of the integrand as a product of conditional probabilities and, if f_i is normalized to unity, one generates random phase-space points $(\mathbf{x}; \mathbf{M}')$ at the initial time 0 (note that, in this context, a virtual particle represents now a set of n phase-space coordinates). These points initialize the trajectories of the particles $\mathbf{x}(y)$ and the exponent, as for the single-body case, gives the probability for a particle to remain over the trajectory provided that the *out-of-trajectory* event rate is γ. This probability filters out these particles, such that the randomly generated out-of-trajectory time is less than τ. If the particle remains in the same trajectory till time τ, it has a contribution to $\langle A \rangle_0(\tau)$ equal to $f_i(\mathbf{x}, \mathbf{M}') A(\mathbf{x}(\tau), \mathbf{M}')$, otherwise it does not contribute at all. Thus, $\langle A \rangle_0(\tau)$ is estimated by the mean value obtained from the N initialized particles.

In the same way, one can proceed further and show that the first order term of the many-body Liouville–Neumann series reads:

$$\langle A \rangle_1(\tau) = \int_0^\infty dt' \int d\mathbf{x} \sum_{\mathbf{M}'=-\infty}^{\infty} f_i(\mathbf{x}, \mathbf{M}') \left\{ \gamma(\mathbf{x}(t')) e^{-\int_0^{t'} \gamma(\mathbf{x}(y))dy} \right\}$$

$$\times \theta_D(\mathbf{x}') \int_{t'}^\infty dt \sum_{\mathbf{M}=-\infty}^{\infty} \left\{ \frac{\Gamma(\mathbf{x}'; \mathbf{M}; \mathbf{M}')}{\gamma(\mathbf{x}(t'))} \right\} \left\{ e^{-\int_{t'}^t \gamma(\mathbf{x}'(y))dy} \right\} A(\mathbf{x}'(t); \mathbf{M}; t) \delta(t - \tau),$$

and, again, a physical interpretation can be given which is a generalization of the single-body case. In particular, now a particle is initialized at $(\mathbf{x}, \mathbf{M}', 0)$ which follows the trajectory until time t' given by the probability density in the first curly brackets. Then, the particle phase-space position is $\mathbf{x}' = (\mathbf{x}(t'); \mathbf{M}'; t')$ and the evolution continues if the particle is still in the simulation domain (otherwise the contribution is zero). A similar interpretation can be given to the term in the next curly bracket which brings the particle from $\mathbf{M}'$ to $\mathbf{M}$ (locally in space at the time t'). Thus, at moment t' the particle initializes the trajectory $(\mathbf{x}'; \mathbf{M})$ and, with the probability given by the exponent in the last curly brackets, remains over the trajectory until time τ.

The first three terms of the Liouville–Neumann series show how to continue with higher order terms [38]. As for the single-body case, the expansion of $\langle A \rangle$ branches and the total value is given by the sum of all branches. We can, thus, equivalently talk in terms of three appearing particles even for the many-body WMC method (note that, in this context, by particle one means a mathematical point defined in a nd-dimensional phase-space), in other words:

$$\frac{\Gamma(\mathbf{x}; \mathbf{M}; \mathbf{M}')}{\gamma(\mathbf{x})} = \left\{ \frac{V_W^+(\mathbf{x}, \mathbf{M} - \mathbf{M}')}{\gamma(\mathbf{x})} \right\} - \left\{ \frac{V_W^-(\mathbf{x}, \mathbf{M} - \mathbf{M}')}{\gamma(\mathbf{M})} \right\} + \left\{ \delta_{\mathbf{M}, \mathbf{M}'} \right\}. \tag{65}$$

According to the last term, the initial parent particle survives and a couple of new signed particles are generated with the first two probabilities. In other words, we generate the first many-body momentum state $\mathbf{M} - \mathbf{M}' = \mathbf{L}$ with probability:

$$\frac{V_W^+(\mathbf{x}, \mathbf{L})}{\gamma(\mathbf{x})},$$

and, with the same probability, we generate another value, say $\mathbf{L}'$, for the second state $\mathbf{M}' - \mathbf{M} = \mathbf{L}'$. In the same way, by exploiting the term $\Gamma(\mathbf{x}; \mathbf{M}; \mathbf{M}')$, it is possible to depict a MC algorithm for the integration of the many-body semi-discrete Wigner equation (60). After any free flight the initial particle creates two new particles with opposite signs and momentum offset (around the initial momentum) equal to $+\mathbf{L}$ and $-\mathbf{L}$ with $\mathbf{L} = \mathbf{M} - \mathbf{M}'$. The initial particle and the created couple represent three contributive terms to the many-body Liouville–Neumann series.

As a concluding remark, one should note that this method implies high scalability of the algorithm (being a MC method). In particular, the scalability does not depend on the number of particles involved in the many-body problem. Indeed, the solution is constructed by an ensemble of field-less Newtonian particles which are *independent* from each other. This represents an important advantage for complex systems where the number of involved bodies can be relatively large.

5.4. Notes on computational complexity

Some comment on the computational complexity of the many-body Wigner MC method are given. It is relatively easy to demonstrate that the complexity of the part of the algorithm dealing with the evolution of the phase-space coordinates of the virtual particles increases linearly with the number of bodies involved [55]. But the calculation of the Wigner kernel (24) is now the bottle neck of the algorithm, as it is equivalent to the calculation of a function defined over a space which dimensions increase exponentially with the number of bodies involved. While this does not represent a problem for non-interacting fermions (where the function $\gamma = \gamma(\mathbf{x}_1, \ldots, \mathbf{x}_n)$ is time-independent, even in the case of entangled particles), it is a severe limitation when all interactions have to be taken into account in a consistent way, since the Coulombic interactions have to be updated at every time step.

6. Applied quantum mechanics in the Wigner formalism

The works of Wigner [11], Moyal [42], Groenewold [65], Dias et al. [58] put the Wigner formulation of quantum mechanics on solid mathematical foundations and allow the description of quantum mechanical systems without the need for wave-functions. As a matter of fact, these systems can be completely described in terms of quasi-distribution functions without recurring to any of the concepts of the Schrödinger formalism. In this section we focus on several quantum systems: the hydrogen atom, the lithium atom, the boron atom, the H_2 molecule, and systems of identical Fermions. We show that it is possible to compute the corresponding Wigner quasi-distribution functions of these systems and, consequently, their spatial probability distributions along with their corresponding macroscopic variables. These are important results. Indeed, on the one hand they clearly show that it is possible to do quantum mechanics without wave-functions. On the other hand, they show how convenient the Wigner formalism is when applied to concrete and practical quantum systems.

6.1. The hydrogen atom

In this section we focus on the hydrogen atom, which has a special significance in quantum mechanics, and show that it is possible to calculate analytically its corresponding Wigner quasi-distribution functions in the $*$-genproblem context. This is the first example showing concretely that it is possible to describe quantum mechanical objects by using quasi-distributions only.
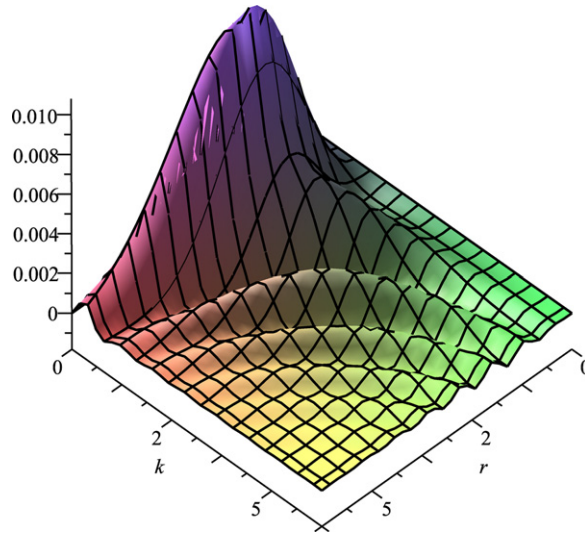
Fig. 2. Wigner quasi-distribution function of the 1s Hydrogen state for $\theta = 0$. Units are chosen so that the Bohr radius is $a = 1$.

As demonstrated in [83], the bound states of the hydrogen atom are analytically expressed as

$$f_W^{nlm}(\mathbf{x}; \mathbf{p}) = \hat{\mathbf{D}}_{nlm}\left(\nabla_{\mathbf{x}}, \frac{\partial}{\partial b_1}, \frac{\partial}{\partial b_2}\right) I(\mathbf{x}, \mathbf{p}, \theta, b_1, b_2)|_{b_1 = b_2 = \frac{1}{na}}, \tag{66}$$

where θ is the angle between the two vector $\mathbf{x}$ and $\mathbf{p}$, a is the Bohr radius, (n, l, m) the principle, the angular momentum and the magnetic quantum numbers respectively,

$$I(\mathbf{x}, \mathbf{p}, \theta, b_1, b_2) = \int_0^1 du \frac{e^{\frac{4iuxp\cos\theta}{\hbar}}}{C(u)} e^{-2xC(u)}, \tag{67}$$

and

$$C(u) = \sqrt{ub_1^2 + (1-u)b_2^2 + 4u(1-u)\left(\frac{p}{\hbar}\right)^2}.$$

The operator $\hat{\mathbf{D}}_{nlm}$ acts on the function $I = I(\mathbf{x}, \mathbf{p}, \theta, b_1, b_2)$ and is defined in detail in [83].

For instance, the 1s state $(n, l, m) = (1, 0, 0)$, the 2s state $(n, l, m) = (2, 0, 0)$, and the 2p$_x$ state $(n, l, m) = (2, 1, 0)$ read respectively

$$f_W^{100}(\mathbf{x}; \mathbf{p}) = \hat{\mathbf{D}}_{100} I(\mathbf{x}, \mathbf{p}, \theta, b_1, b_2)|_{b_1 = b_2 = \frac{1}{a}}$$

$$f_W^{200}(\mathbf{x}; \mathbf{p}) = \hat{\mathbf{D}}_{200} I(\mathbf{x}, \mathbf{p}, \theta, b_1, b_2)|_{b_1 = b_2 = \frac{1}{2a}}$$

$$f_W^{210}(\mathbf{x}; \mathbf{p}) = \hat{\mathbf{D}}_{210} I(\mathbf{x}, \mathbf{p}, \theta, b_1, b_2)|_{b_1 = b_2 = \frac{1}{2a}},$$

with

$$\hat{\mathbf{D}}_{100} = \frac{2e^{\frac{-2irp\cos\theta}{\hbar}}}{\pi^3 a^3} \frac{\partial^4}{\partial b_1^2 \partial b_2^2}$$

$$\hat{\mathbf{D}}_{200} = -\frac{e^{\frac{-2irp\cos\theta}{\hbar}}}{4\pi^3 a^3}\left[\frac{\partial}{\partial b_1} - b_1\frac{\partial^2}{\partial b_1^2}\right]\left[\frac{\partial}{\partial b_2} - b_2\frac{\partial^2}{\partial b_2^2}\right]$$

$$\hat{\mathbf{D}}_{210} = \frac{2e^{\frac{2irp\cos\theta}{\hbar}}}{(2\pi)^3 a^5}\left(\frac{\partial}{\partial b_1}\frac{1}{2b_1}\frac{\partial}{\partial b_1}\right)\left(\frac{\partial}{\partial b_2}\frac{1}{2b_2}\frac{\partial}{\partial b_2}\right)\left(\frac{\partial^2}{\partial x^2} + 4i\frac{p_z}{\hbar}\frac{\partial}{\partial x}\right)e^{-4irp\cos\theta/\hbar}, \tag{68}$$

and the 1s bound state Wigner function f_W^{100} is shown in Figs. 2 and 3 for $\theta = 0$ and $\theta = \frac{\pi}{2}$ respectively.
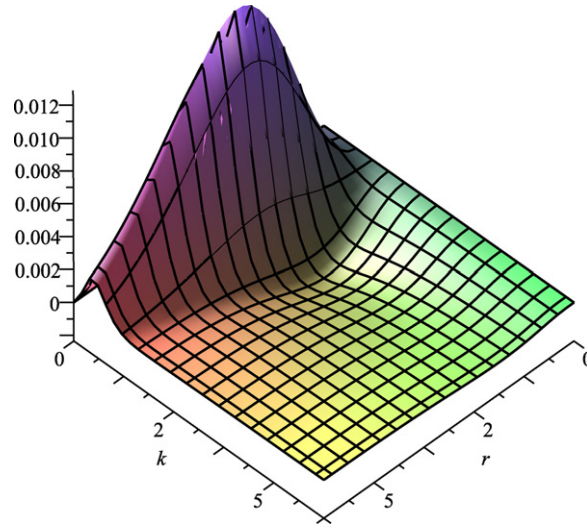
Fig. 3. Wigner quasi-distribution function of the 1s Hydrogen state for $\theta = \frac{\pi}{2}$. Units are chosen so that the Bohr radius is $a = 1$.

In particular, the case $\theta = \frac{\pi}{2}$ corresponds to a classical orbit [83] and it is presented in Fig. 3. It is interesting to note that the corresponding Wigner function is non-negative in any point of the phase-space, i.e. it behaves as a proper distribution function. Instead, negative values appear for the case $\theta = 0$ as one clearly sees from Fig. 2, a clear indication that we are in the presence of dominant quantum effects. One also notes that the quasi-distribution functions represented in Figs. 2 and 3 give more information on the state of the electron in the potential generated by the nucleus. For example, one clearly sees that the peak in the spatial position corresponds to $x = a$, i.e. the highest probability of finding the electron is on a orbital which radius is equal to the Bohr radius, and the energy peak is in proximity of the ground state of the system (as expected). The same conclusions can be inferred in the Schrödinger formalism but in terms of a rather more abstract perspective.

6.2. The lithium and boron atoms

We now focus on the simulation of the stationary states for the lithium and boron atoms. The lithium atom consists of one nucleus with charge $+3e$ and 3 electrons with negative charge $-e$, interacting with the nucleus and each other. The boron atom consists of one nucleus with charge $+5e$ and 5 electrons.

For both elements, we apply the Wigner MC DFT method and simulate the system of Eq. (58). In particular, the experiment for lithium and boron consists of computing the stationary configuration of electrons starting from a non-stationary initial condition, thus testing the capability of the method to stay in a stationary regime. These are non-trivial experiments since the Wigner MC method is based on Newtonian particles constantly moving as free-field objects. Reaching a stationary regime and keeping it for a long simulation time is a clear indication of the robustness and reliability of the method.

We choose to simulate the lithium atom as its orbitals are known to have a spherical symmetry. The boron atom, instead, is chosen because the symmetry is not valid anymore for its 2p orbital, thus representing a more difficult numerical task. In both experiments the nuclei are modeled as non-screened Coulombic charges and, in order to avoid singularities in the numerical treatment of the nuclei, we utilize the following modified potential [84]:

$$V_{ion}(\mathbf{x}) = \frac{Ze}{4\pi\epsilon_0 \left((\mathbf{x} - \mathbf{x}_{ion})^2 + \frac{1}{2}a^2\right)^{\frac{1}{2}}}, \tag{69}$$

where, as usual, Z is the atomic number, a is the Bohr radius and $\mathbf{x}_{ion}$ is the position of the center of the nucleus. One should note that this choice does not represent a restriction for the method and one could use any other available mathematical model, such as pseudo-potential models, etc.

The initial conditions for the Wigner functions are represented by non-stationary states which are directly proportional to the electron density of a hydrogenic state in space and Gaussian in energy (around some initial energy E_0). In particular, for the lithium atom (2 electrons in 1s state and 1 electron in 2s state), the initial conditions for the 3 electrons are:

$$f_w^{1s}(\mathbf{x}; \mathbf{p}; 0) = A_{1s} e^{\frac{-\left(\frac{p^2}{2m} - E_0\right)}{\sigma_E^2}} e^{-\frac{|\mathbf{x} - \mathbf{x}_{ion}|}{a}} \tag{70}$$
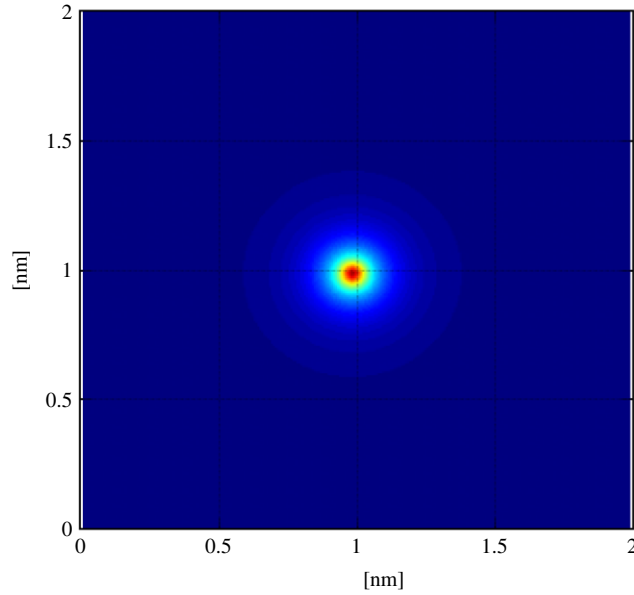
Fig. 4. Nucleus potential created by a lithium nucleus.

(two times) and

$$f_w^{2s}(\mathbf{x}; \mathbf{p}; 0) = A_{2s} e^{-\frac{\left(\frac{p^2}{2m} - E_0\right)}{\sigma_E^2}} e^{-\frac{|\mathbf{x} - \mathbf{x}_{ion}|}{a}} \left(1 - \frac{|\mathbf{x} - \mathbf{x}_{ion}|}{a}\right), \tag{71}$$

where A_{1s} and A_{2s} are normalization constants (the density probability corresponding to every Wigner quasi-distribution is normalized to unity, i.e. one electron per equation) and σ_E is the dispersion in energy. For the boron atom, the initial conditions consist of two electrons in the state (70), two electrons in the state (71) and one electron in an initial state corresponding to a density directly proportional to a 2p state:

$$f_w^{2p}(\mathbf{x}; \mathbf{p}; 0) = A_{2p} e^{-\frac{\left(\frac{p^2}{2m} - E_0\right)}{\sigma_E^2}} e^{-\frac{|\mathbf{x} - \mathbf{x}_{ion}|}{a}} (\mathbf{x} - \mathbf{x}_{ion})^2. \tag{72}$$

Both systems are evolved in time until a stationary solution is reached.

For the sake of simplicity, we choose the following (LDA) exchange–correlation functional [75] which, in atomic units, reads:

$$U_{xc}[\rho](\mathbf{x}) = -\frac{1}{\pi} \left[3\pi^2 \rho(\mathbf{x})\right]^{\frac{1}{3}}. \tag{73}$$

One should note that our method is not limited by the choice of any particular exchange–correlation functional and other models for $U_{xc}[\rho]$ can be utilized.

The results for the lithium atom are reported in Figs. 4–6. In particular, Fig. 4 shows the potential generated by the nucleus. It is clear from this last figure how the dynamics of the wave packet is affected in proximity of the nucleus. As a matter of fact, a zero node can be observed in the position corresponding to the nucleus, indicating that no couple of signed particles is generated in that area. Figs. 5 and 6, instead, show the electron probability densities corresponding to time equal to 50 attoseconds, for the 1s and 2s states respectively. The electron states have evolved towards a stationary state and do not change any longer.

The results concerning the boron atom are reported in Figs. 7–9. In particular, Figs. 7–9 show the electron probability densities corresponding to time equal to 50 attoseconds, for the 1s, 2s and 2p states respectively. Again, the system converges to a stationary regime. Furthermore, the 2p orbital, not spherically symmetric, remains stationary in time.

6.3. The H₂ molecule

We now simulate, by using the Wigner MC DFT method, a system consisting of two hydrogen atoms (two fixed positive nuclei and two electrons in motion) in two different configurations. Initially we suppose that the two nuclei are far apart and in a second time we put them closer by a distance comparable to one Angstrom. Given enough time, both configurations evolve towards a stationary regime. In particular, the appearance of a chemical bond is observable in the second
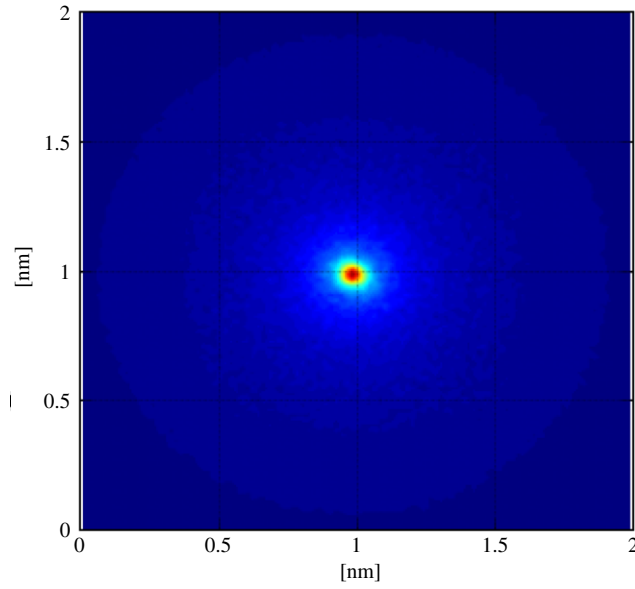
Fig. 5. Density of an electron in lithium 1s orbital.
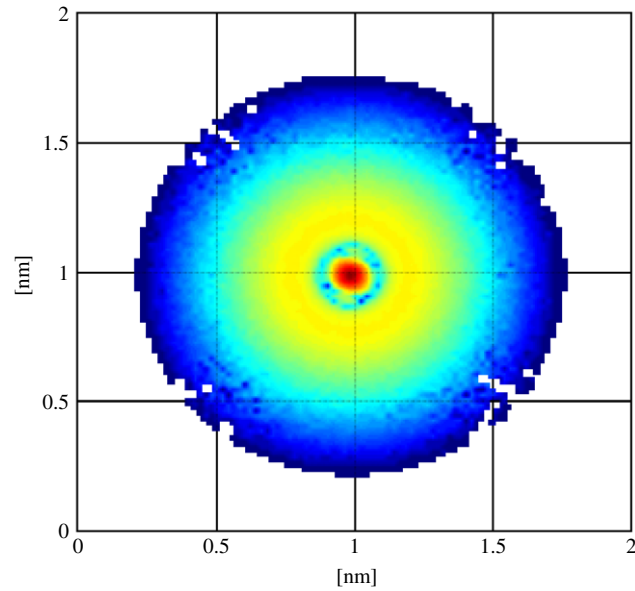

Fig. 6. Density of an electron in lithium 2s orbital (logarithmic scale).

configuration. For the sake of completeness, the Wigner MC DFT solutions are compared with the standard DFT based on the (Schrödinger-) Kohn–Sham system which reads (for two interacting electrons):

$$i\hbar \frac{\partial \Phi_1}{\partial t}(\mathbf{x}, t) = \left(-\frac{\hbar^2 \nabla^2}{2m} + U_{\text{eff}}(\mathbf{x})\right) \Phi_1(\mathbf{x}, t)$$

$$i\hbar \frac{\partial \Phi_2}{\partial t}(\mathbf{x}, t) = \left(-\frac{\hbar^2 \nabla^2}{2m} + U_{\text{eff}}(\mathbf{x})\right) \Phi_2(\mathbf{x}, t),$$

(74)

where the effective potential U_{eff} is given by (57), U_{xc} is the (LDA) functional (73), and the Coulombic ions are expressed by (69). The simulation technique for each equation in (74) is based on the time implicit finite difference method proposed in [85].

The results for a system made of two far apart hydrogen atoms are reported in Figs. 10, 12, 14 and 16. In particular, Fig. 16 shows a comparison with the standard DFT method. The initial electron density is shown in Fig. 12 while the potential is
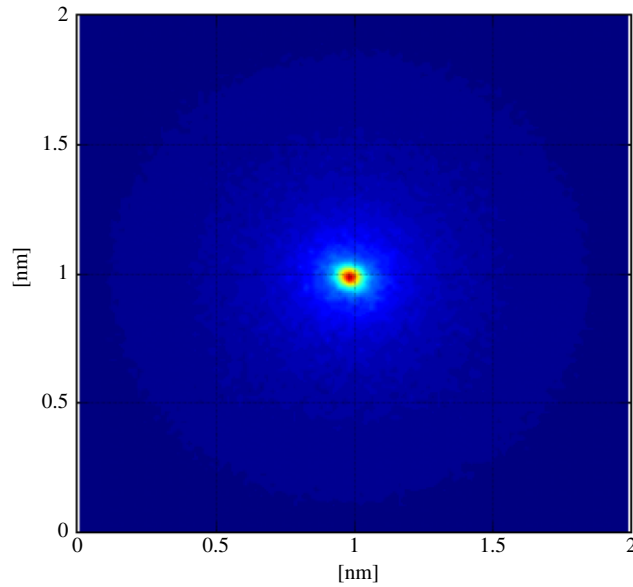
Fig. 7. Density of an electron in boron 1s orbital.
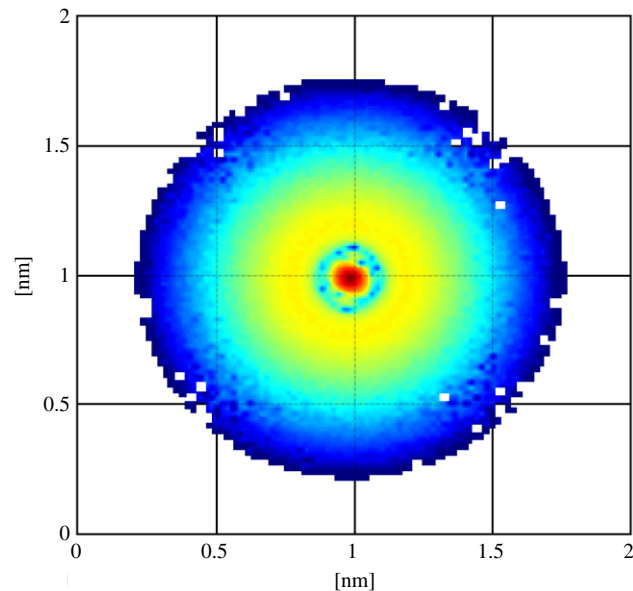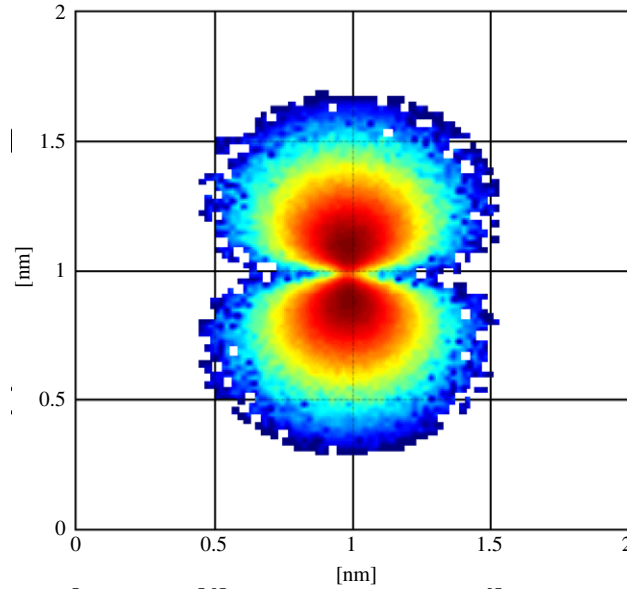

Fig. 8. Density of an electron in boron 2s orbital (logarithmic scale).

shown in Fig. 10. The system is evolved in time until 50 attoseconds and a stationary solution is already reached at about 4 attoseconds. The electron probability density at 50 attoseconds is shown in Fig. 14. It is clear that the solution is evolving towards a couple of non-interacting s-shape orbitals. This is qualitatively in accordance with the fact that the system is expected to reach a stationary regime, if reasonable initial conditions are imposed (not too far from equilibrium). The cuts for various densities at 50 attoseconds are shown in Fig. 16 compared to the standard DFT results. The two single-electron densities are clearly s-shape non-interacting orbitals. Furthermore, the solution for the total density is quantitatively in agreement with the standard DFT. The resemblance is striking especially if one thinks that the two methods are profoundly different (i.e. MC vs. finite differences).

Now the two hydrogen atoms are positioned relatively closer. In this case, the electron–electron interactions are expected to be important due to the proximity of the nuclei. The system is evolved in time until 50 attoseconds and a stationary solution is reached at about 5 attoseconds already. The results of this experiment are reported in Figs. 11, 13, 15 and 17. In particular, Fig. 13 shows the initial electron probability density in the total potential of Fig. 11. The corresponding electron density is shown in Fig. 15. A bond is formed between the two atoms as part of the electron density is spread in the area

**Fig. 9.** Density of an electron in boron 2p orbital (logarithmic scale).
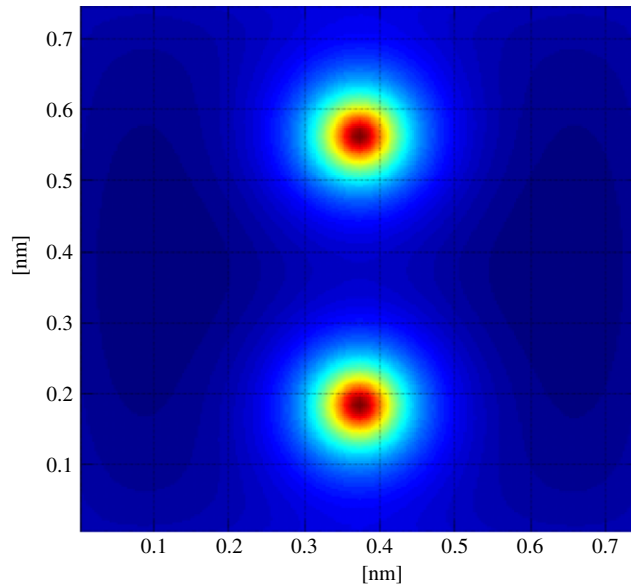
Fig. 10. Nuclei potential created by two distant hydrogenic atoms.

between the two nuclei. This is clearly shown in Fig. 17 where the two single electron probability densities (dotted curves) and the total density (o− curve) are reported along with the total density obtained from the standard DFT. Finally, one notes that the solution for the total density is quantitatively in agreement with the standard DFT. Even in this case, the resemblance is self-evident.

6.4. Systems of Fermions and the Pauli exclusion principle

We now apply the ab-initio many-body Wigner MC method to a system of two interacting indistinguishable fermions and show that the Pauli exclusion principle is naturally taking place into the evolution of the system in the many-body Wigner formalism. The way it is embedded is by means of the initial conditions which have to correspond to a system of fermions, i.e. the initial Wigner function is calculated from an antisymmetric wave-function.
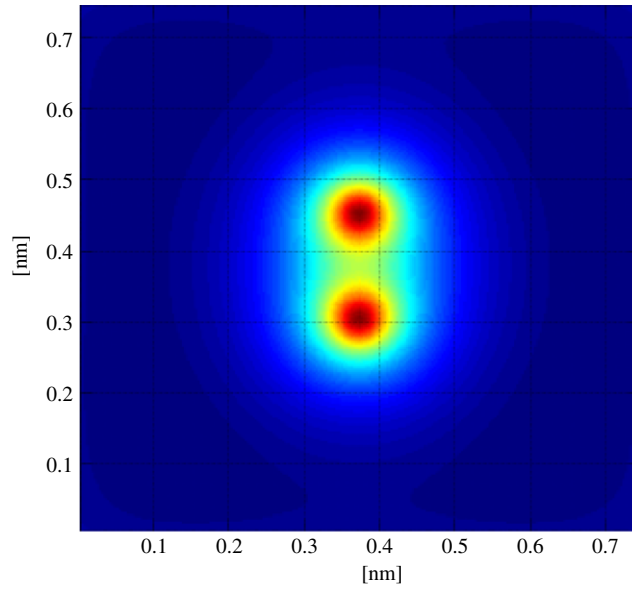
Fig. 11. Nuclei potential created by two close hydrogenic atoms.
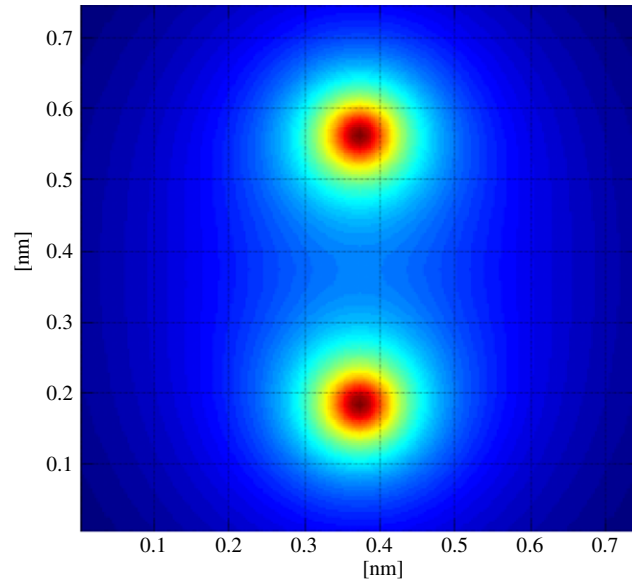
Fig. 12. Initial electron density corresponding to two Gaussian wave packets in proximity of two distant hydrogenic nuclei.

In particular, the system simulated consists of two identical electrons, trapped in a one-dimensional box, interacting with each other through their Coulombic potential. The system starts from the initial conditions
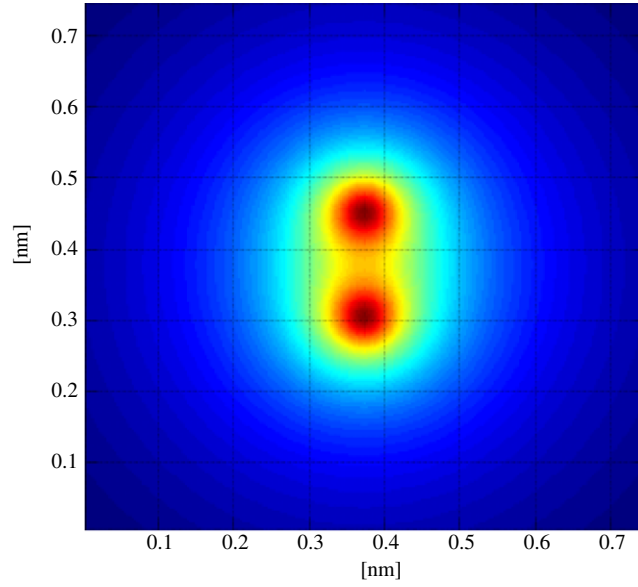
$$f_W^0(x_1, x_2; p_1, p_2) = \frac{1}{(\hbar\pi)^2} \int dx_1' dx_2' e^{-\frac{i}{\hbar}(x_1'p_1 + x_2'p_2)} \times \Psi_0\left(x_1 + \frac{x_1'}{2}, x_2 + \frac{x_2'}{2}\right) \Psi_0^*\left(x_1 - \frac{x_1'}{2}, x_2 - \frac{x_2'}{2}\right),$$
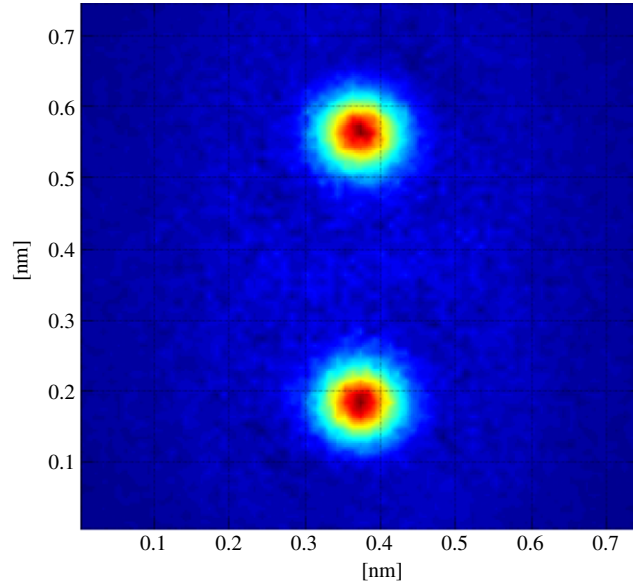
with

$$\Psi_0(x_1, x_2) = \begin{vmatrix} \phi_1(x_1) & \phi_2(x_2) \\ \phi_1(x_2) & \phi_2(x_2) \end{vmatrix},$$

(Slater determinant, i.e. antisymmetric wave-function) and

$$\phi_1(x) = N_1 e^{-\frac{1}{2}\left(\frac{x - x_1^0}{\sigma}\right)^2} e^{ip_1^0 x},$$

Fig. 13. Initial electron density corresponding to two Gaussian wave packets in proximity of two close Hydrogenic nuclei.
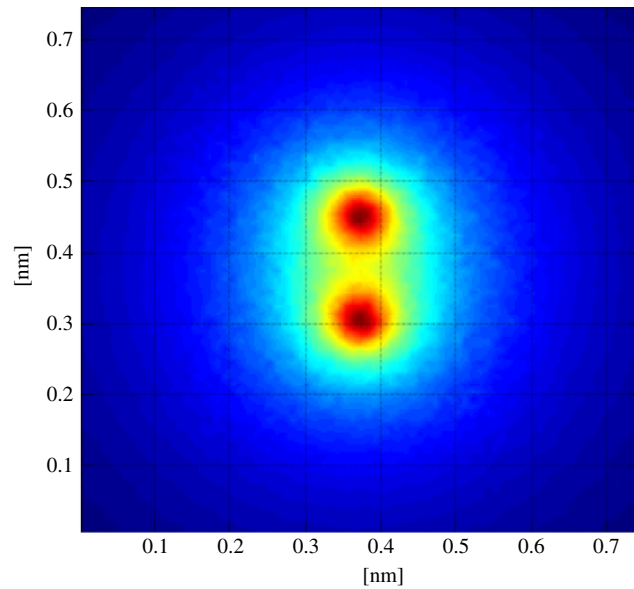

Fig. 14. Electron density at 0.05 fs. The two packets tends to two separated s-shape orbitals.

$$\phi_2(x) = N_2 e^{-\frac{1}{2}\left(\frac{x - x_2^0}{\sigma}\right)^2} e^{i p_2^0 x},$$

where N_1 and N_2 are normalization constants, x_1^0 and x_2^0 are the initial central positions, p_1^0 and p_2^0 are the initial momenta, for the first and the second wave-packet respectively, and σ the initial dispersion of the wave-packets. In this particular experiment, the values $x_1^0 = 20$ nm, $x_2^0 = 30$ nm, $p_1^0 = +2\Delta p$, $p_2^0 = -2\Delta p$, and $\Delta p = \frac{\pi}{\hbar L_C}$ with $L_C = 20$ nm, have been used and the evolution is performed until time 3.5 fs (a very long final time if compared to the typical time scale being of the order of a few attoseconds in this context). Finally, the total length of the spatial domain is equal to 150 nm.

The results of the simulations are reported in Figs. 18 and 19. showing the evolution of the quantity $\int d\mathbf{x}_1 d\mathbf{p}_1 f_W(\mathbf{x}_1, \mathbf{x}_2; \mathbf{p}_1, \mathbf{p}_2; t) + \int d\mathbf{x}_2 d\mathbf{p}_2 f_W(\mathbf{x}_1, \mathbf{x}_2; \mathbf{p}_1, \mathbf{p}_2; t)$ in the phase-space at time 0 fs, 1 fs, 2.5 fs and 3.5 fs respectively.

The two particles start with the same energy but with opposite momenta, Fig. 18 (top). They proceed one from right to left, the other from left to right feeling their repulsive Coulombic potential, Fig. 18 (bottom). At time 2.5 fs, Fig. 19 (top), a Fermi (or exchange–correlation) hole is clearly visible. This is equivalent to *pinching* two electrons with same energy against each

Fig. 15. Electron density at 0.05 fs. A bond is formed between the two atoms.
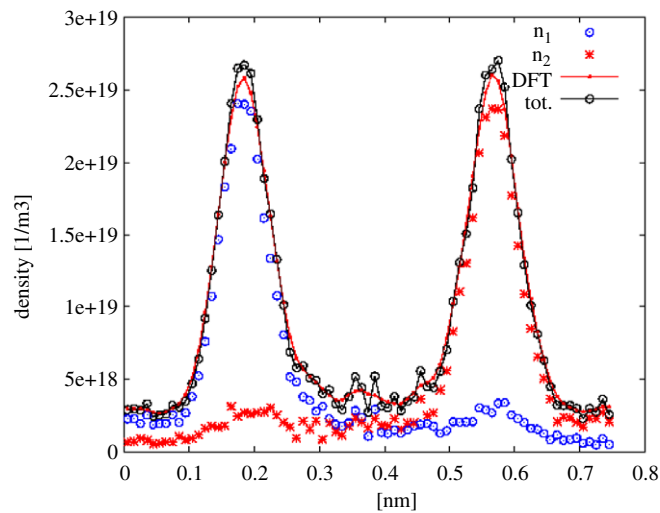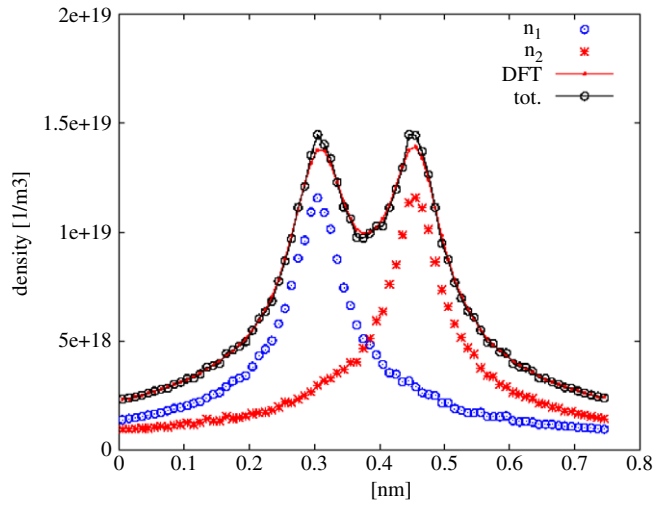

Fig. 16. Cut along the nuclei axis of the electron density at 0.05 fs. The two packets (dotted curves) tends to two separated s-shape orbitals. A good agreement is achieved between our proposed model based on WMC, (black) $o-$ line, and the standard DFT, (red) $.-$ line. (For interpretation of the references to colour in this figure legend, the reader is referred to the web version of this article.)

other and, accordingly, a lower probability is developed in the central area of the phase-space, preventing the two particles to be in the same position with the same energy or, in other words, to be in the same orbital. This is a clear indication of the presence of the Pauli exclusion principle. Eventually, as the evolution proceeds in time, the Fermi hole disappears, Fig. 19 (bottom).

6.5. Computational aspects

The simulator used to obtain the results presented in this paper is a modified version of Archimedes, the GNU package for the simulation of carrier transport in semiconductor devices [86] which was first released in 2005 under the GNU Public License (GPL). In this particular project, named *nano-archimedes*, our aim has been to develop a full quantum time-dependent simulator. The code is entirely developed in C and optimized to get the best performance from the hardware. It can run on parallel machines using the OpenMP standard library. The results of the present version are posted on the nano-archimedes website, dedicated to the simulation of quantum systems [68]. The source code is available as well.

Fig. 17. Cut along the atoms direction of the electron density at 0.05 fs. The two packets form a bond between the two Hydrogenic atoms. A good agreement is achieved between our proposed model based on WMC, (black) o− line, and the standard DFT, (red) .− line. (For interpretation of the references to colour in this figure legend, the reader is referred to the web version of this article.)
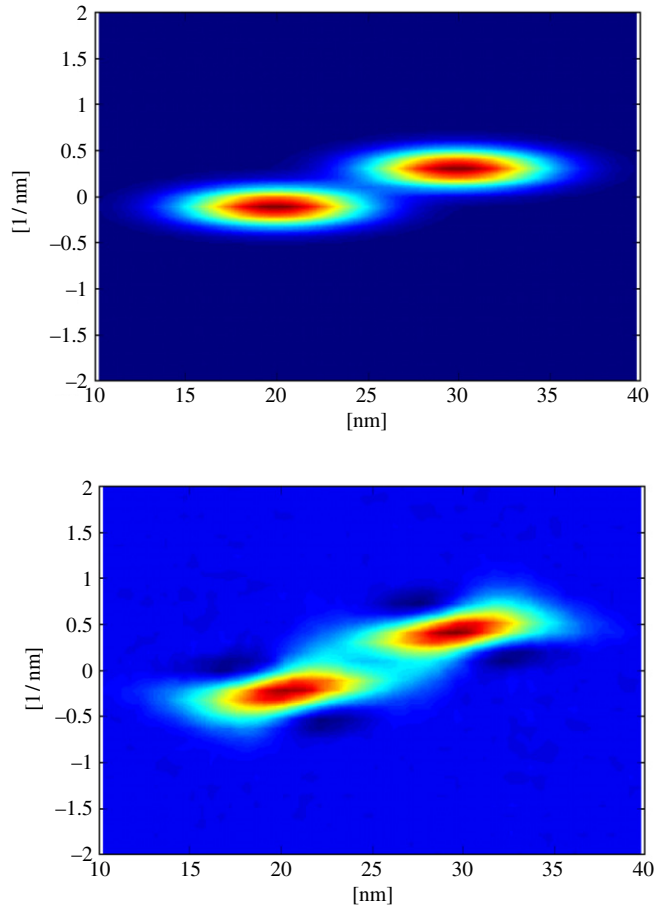
Fig. 18. Time-dependent evolution of the quantity $\int d\mathbf{x}_1 d\mathbf{p}_1 f_W(\mathbf{x}, \mathbf{p}, t) + \int d\mathbf{x}_2 d\mathbf{p}_2 f_W(\mathbf{x}, \mathbf{p}, t)$ at time 0 fs (top) and 1 fs (bottom). The *x*- and *y*-axes refer to position and momentum respectively.

The results have been obtained using the HPC cluster deployed at the Institute of Information and Communication Technologies of the Bulgarian Academy of Sciences. This cluster consists of two racks which contain HP Cluster Platform
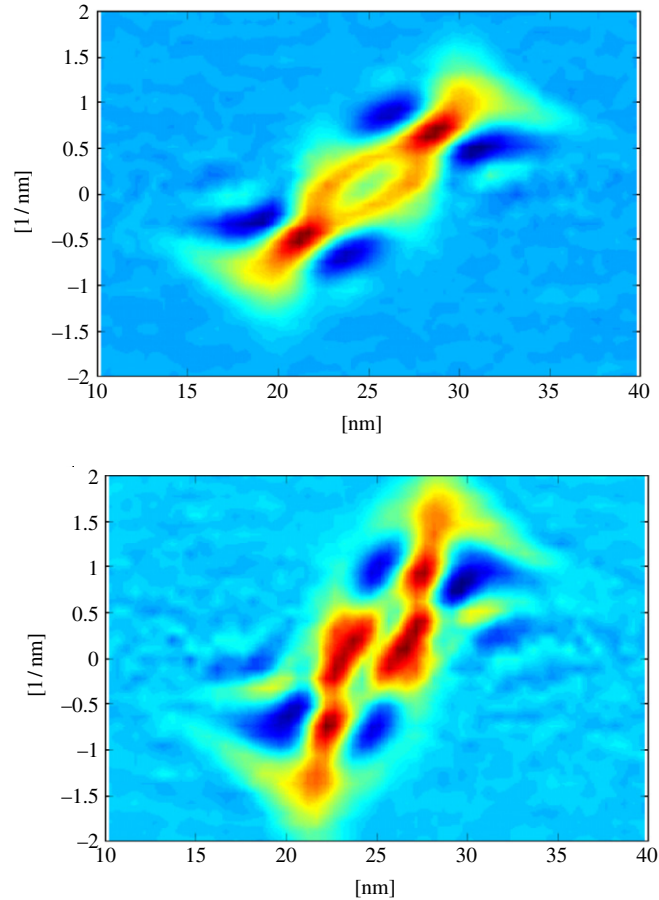
Fig. 19. Time-dependent evolution of the quantity $\int d\mathbf{x}_1 d\mathbf{p}_1 f_W(\mathbf{x}, \mathbf{p}, t) + \int d\mathbf{x}_2 d\mathbf{p}_2 f_W(\mathbf{x}, \mathbf{p}, t)$ at time 2.5 fs (top) and 3.5 fs (bottom). The formation of a Fermi hole (also known as an exchange–correlation hole), due to the Pauli exclusion principle, is clearly visible at time 2.5 fs (top). Eventually the hole disappears (3.5 fs) as the system evolves (bottom). The x- and y-axes refer to position and momentum respectively.

Express 7000 enclosures with 36 blades BL 280c with dual Intel Xeon X5560 @ 2.8 GHz (total 576 cores), 24 GB RAM per blade. There are 8 storage and management controlling nodes 8 HP DL 380 G6 with dual Intel X5560 @ 2.8 GHz and 32 GB RAM. All these servers are interconnected via non-blocking DDR Infiniband interconnect at 20 Gbps line speed. The theoretical peak performance is 3.23 Tflops.

7. Summary and future developments

In this review endeavor, we have introduced and explained the Wigner formulation of quantum mechanics. We have shown that it is mathematically equivalent to the Schrödinger formalism although it allows the treatment of quantum systems in terms of (quasi-)distribution functions only without involving the concept of wave-functions. We also have shown the mathematical properties a quasi-distribution must have to describe a *physical* system. In a second time, we have introduced a Monte Carlo method for the simulation of the single-body Wigner equation. This method has been, then, extended to the frameworks of density functional theory and ab-initio methods for the time-dependent simulation of the quantum many-body problem. This represents an important achievement as Monte Carlo methods allow a drastically deep level of parallelization, opening the way towards time-dependent, full-quantum simulations of complex and relatively large, correlated and non-correlated, chemical and physical systems. Moreover, we have shown how the Wigner formalism can be applied in practical calculations. As a first example, we have shown that the time-independent Wigner equation (∗-genproblem) can be utilized to study, and intuitively understand, the states of a hydrogen atom. As a second example, we have applied the Wigner MC DFT method to the simulation of lithium and boron atoms. Afterwards, the same method has been applied to the simulation of a H_2 molecule in two different configurations. Finally, we applied the ab-initio many-body Wigner MC method to a system of entangled particles. These applications clearly demonstrate that it is possible to simulate practical quantum systems and get insights which cannot be reached by other formalisms of quantum mechanics.

Clearly, still a lot remains to be explored from both a theoretical and numerical point of view but we think that, based on the promising results reported in this review, it is a very exciting time for those scientists who want to use an alternative

approach to the standard formulation of quantum mechanics, accessing the realm of time-dependent quantum simulations of complex objects.

Acknowledgment

References

[1] B. Stewart, An account of some experiments on radiant heat, Trans. R. Soc. Edinburgh 22 (1858) 1–20.
[2] H.R. Hertz, Ueber einen einfluss des ultravioletten Lichtes auf die electrische entladung, Ann. Phys. 267 (1887) 983–1000.
[3] M. Planck, Entropy and temperature of radiant heat, Ann. Phys. 1 (1900) 719–737.
[4] A. Einstein, Concerning an heuristic point of view toward the emission and transformation of light, Ann. Phys. 17 (1905) 132–148.
[5] N. Bohr, On the constitution of atoms and molecules, Phil. Mag. 26 (1913) 1.
[6] E. Schrödinger, Quantisierung als Eigenwertproblem, Ann. Phys. 385 (1926) 437–490.
[7] M. Born, On the quantum mechanics of collisions, in: J.A. Wheeler, W.H. Zurek (Eds.), Quantum Theory and Measurement, Section I.2, Princeton University Press, Princeton, New Jersey, 1983.
[8] H. Everett, Relative state formulation of quantum mechanics, Rev. Modern Phys. 29 (1957) 454–462.
[9] D. Bohm, A suggested interpretation of the quantum theory in terms of 'hidden variables' I, Phys. Rev. 85 (1952) 166–179.
[10] E. Nelson, Derivation of the Schrödinger equation from Newtonian mechanics, Phys. Rev. 150 (1966) 1079–1085.
[11] E. Wigner, On the quantum correction for thermodynamic equilibrium, Phys. Rev. 40 (1932) 749.
[12] R.P. Feynman, Space–time approach to non-relativistic quantum mechanics, Rev. Modern Phys. 20 (1948) 367.
[13] L.V. Keldysh, Zh. Eksp. Teor. Fiz., Sov. Phys. JETP 20 (1965).
[14] E.A. Remler, Ann. Phys. 95 (1975) 455.
[15] E.A. Remler, Ann. Phys. 136 (1981) 293.
[16] E.A. Remler, A.P. Sathe, Ann. Phys. 91 (1975) 295.
[17] E.A. Remler, A.P. Sathe, Phys. Rev. C 18 (1978) 2293.
[18] R.C. Brown, E.J. Heller, Classical trajectory approach to photodissociation: The Wigner method, J. Chem. Phys. 75 (1981) 186.
[19] B.C. Eu, J. Chem. Phys. 54 (1971) 559.
[20] B.C. Eu, J. Chem. Phys. 63 (1975) 298.
[21] E.J. Heller, J. Chem. Phys. 65 (1976) 1289.
[22] E.J. Heller, J. Chem. Phys. 67 (1977) 3339.
[23] H.W. Lee, M.O. Scully, J. Chem. Phys. 73 (1980) 2238.
[24] J.R.N. Miles, J.S. Dahler, J. Chem. Phys. 52 (1970) 616.
[25] P. Carruthers, F. Zachariasen, Quantum collision theory with phase-space distributions, Rev. Modern Phys. 55 (1983) N. 1.
[26] W.P. Schleich, Quantum Optics in Phase Space, Wiley, 2001.
[27] W.H. Zurek, Sub-Planck structure in phase space and its relevance for quantum decoherence, Nature 412 (2001) 712.
[28] D. Querlioz, P. Dollfus, The Wigner Monte Carlo Method for Nanoelectronic Devices—A Particle Description of Quantum Transport and Decoherence, ISTE-Wiley, 2010.
[29] L. Shifren, D.K. Ferry, Particle Monte Carlo simulation of Wigner function tunneling, Phys. Lett. A 285 (2001) 217–221.
[30] L. Shifren, D.K. Ferry, A Wigner function based ensemble Monte Carlo approach for accurate incorporation of quantum effects in device simulation, J. Comp. Electr. 1 (2002) 55–58.
[31] L. Shifren, D.K. Ferry, Wigner function quantum Monte Carlo, Physica B 314 (2002) 72–75.
[32] M. Van de Put, M. Thewissen, W. Magnus, B. Soree, J.M. Sellier, Spectral force approach to solve the time-dependent Wigner-Liouville equation, in: Proceedings of the 17th International Workshop on Computational Electronics, 2014.
[33] O. Jonasson, I. Knezevic, Coulomb-driven Terahertz-frequency intrinsic current oscillations in a double-barrier tunneling structure, Phys. Rev. B 90 (2014) 165415.
[34] U. Ravaioli, M. Osman, W. Potz, N. Kluksdahl, D. Ferry, Investigation of ballistic transport through resonant tunneling quantum wells using Wigner function approach, Physica B 134 (1985) 36–40.
[35] J. Garcia-Garcia, F. Martin, X. Oriols, J. Sune, Quantum Monte Carlo simulation of resonant tunneling diodes based on the Wigner distribution function formalism, Appl. Phys. Lett. 73 (1998) 3539.
[36] C. Jacoboni, A. Bertoni, P. Bordone, R. Brunetti, Wigner-function formulation for quantum transport in semiconductors: Theory and Monte Carlo approach, Math. Comput. Simul. 55 (2001) 67–78.
[37] J.M. Sellier, I. Dimov, A Wigner Monte Carlo approach to density functional theory, J. Comput. Phys. 270 (2014) 265–277.
[38] J.M. Sellier, I. Dimov, The Many-body Wigner Monte Carlo method for time-dependent ab-initio quantum simulations, J. Comput. Phys. 273 (2014) 589–597.
[39] J.M. Sellier, I. Dimov, Wigner–Boltzmann Monte Carlo method applied to electron transport in the presence of a single dopant, Comput. Phys. Comm. (2014).
[40] J.M. Sellier, I. Dimov, A Wigner approach to the study of wave packets in ordered and disordered arrays of dopants, Physica A (2014).
[41] J.M. Sellier, S.M. Amoroso, M. Nedjalkov, S. Selberherr, A. Asenov, I. Dimov, Electron dynamics in nanoscale transistors by means of Wigner and Boltzmann approaches, Physica A (2014).
[42] J.E. Moyal, Quantum mechanics as a statistical theory, Proc. Cam. Phil. Soc. 45 (1949).
[43] L.G. Lutterbach, L. Davidovich, Method for direct measurement of the Wigner function in cavity QED and ion traps, Phys. Rev. Lett. 78 (1997) 2547.
[44] U. Leonhardt, Measuring the Quantum State of Light, Cambridge University Press, 1997.
[45] D. Leibfried, T. Pfau, C. Monroe, Shadows and mirrors: Reconstructing quantum states of atom motion, Phys. Today (1998).
[46] I. Dimov, Monte Carlo Methods for Applied Scientists, World Scientific, 2008.
[47] N. Metropolis, S. Ulam, The Monte Carlo method, J. Amer. Statist. Assoc. 44, 247 (1949) 335–341.
[48] G. de Buffon, Essai d'Arithmétique Morale, Suppl. Hist. Nat. 4 (1777).
[49] C. Jacoboni, L. Reggiani, The Monte Carlo method for the solution of charge transport in semiconductors with applications to covalent materials, Rev. Modern Phys. 55 (3) (1983) 645.
[50] I. Dimov, Monte Carlo algorithms for linear problems, Pliska Stud. Math. Bulgar. 13 (1997) 57–77.
[51] J. Garcia-Garcia, F. Martin1, X. Oriols, J. Sune, Quantum Monte Carlo simulation of resonant tunneling diodes based on the Wigner distribution function formalism, Appl. Phys. Lett. 73 (1998) 3539.
[52] C. Jacoboni, A. Bertoni, P. Bordone, R. Brunetti, Wigner-function formulation for quantum transport in semiconductors: theory and Monte Carlo approach, Math. Comput. Simul. 55 (2001) 67–78.
[53] M. Nedjalkov, P. Schwaha, S. Selberherr, J.M. Sellier, D. Vasileska, Wigner quasi-particle attributes—an asymptotic perspective, Appl. Phys. Lett. 102 (2013) 163113.

J.M. Sellier et al. / Physics Reports 577 (2015) 1–34

[54] J.M. Sellier, M. Nedjalkov, I. Dimov, S. Selberherr, A benchmark study of the Wigner Monte-Carlo method, Monte Carlo Methods and Applications, De Gruyter, 2014. http://dx.doi.org/10.1515/mcma-2013-0018.
[55] I. Dimov, T. Gurov, Monte Carlo algorithm for solving integral equations with polynomial non-linearity. Parallel implementation, Pliska Stud. Math. Bulgar. 13 (2000) 117–132.
[56] K. Schram, B.R. Nijboer, The Wigner distribution function for systems of Bosons and Fermions, Physica 25 (2006) 733–741.
[57] R.C. Balescu, Equilibrium and Non-equilibrium Statistical Mechanics, Wiley, 1975.
[58] N.C. Dias, J.N. Prata, Admissible states in quantum phase space, Ann. Physics 313 (2004) 110–146.
[59] L.D. Landau, L.M. Lifshitz, Quantum Mechanics: Non-Relativistic Theory, vol. 3, 1976.
[60] J. von Neumann, Wahrscheinlichkeitstheoretischer Aufbau der Quantenmechanik, Göttinger Nachr. (1927) 245–272.
[61] J.M. Sellier, I. Dimov, On the simulation of indistinguishable fermions in the many-body Wigner formalism, J. Comput. Phys. 280 (2015) 287–294.
[62] E. Cancellieri, P. Bordone, A. Bertoni, G. Ferrari, C. Jacoboni, Wigner function for identical particles, J. Comput. Electr. 3 (2004) 411–415.
[63] E. Cancellieri, P. Bordone, C. Jacoboni, Effect of symmetry in the many-particle Wigner function, Phys. Rev. B 76 (2007) 214301.
[64] H. Weyl, Quantenmechanik und Gruppentheorie, Z. Phys. 46 (1927).
[65] H. Groenewold, On the principles of elementary quantum mechanics, Physica 12 (1946) 405.
[66] V.I. Tatarskii, Sov. Phys. Usp 26 (1983) 311.
[67] M. Nedjalkov, H. Kosina, S. Selberherr, Ch. Ringhofer, D.K. Ferry, Unified particle approach to Wigner-Boltzmann transport in small semiconductor devices, Phys. Rev. B 70 (2004) 115319.
[68] J.M. Sellier, nano-archimedes, www.nano-archimedes.com, 2014 (accessed 24.03.14).
[69] J.M. Sellier, I. Dimov, A sensitivity study of the Wigner Monte Carlo method, J. Comput. Appl. Math. 277 (2015) 87–93.
[70] J.M. Sellier, M. Nedjalkov, I. Dimov, S. Selberherr, The role of annihilation in a Wigner Monte Carlo approach, in: I. Lirkov, S. Margenov, J. Wasniewski (Eds.), in: Large-Scale Scientific Computing, Lecture Notes in Computer Sciences, vol. 8353, Springer, 2014.
[71] E. Fermi, Un metodo statistico per la determinazione di alcune prioprietà dell'atomo, Rend. Accad. Naz. Lincei 6 (1927) 602–607.
[72] L.H. Thomas, The calculation of atomic fields, Proc. Camb. Phil. Soc. 23 (1927) 542–548.
[73] J.C. Slater, A simplification of the Hartree–Fock method, Phys. Rev. 81 (1951) 385–390.
[74] D.R. Hartree, The wave mechanics of an atom with a non-coulomb central field. Part i—theory and methods, Proc. Camb. Phil. Soc. 24 (1928) 89–110.
[75] P. Hohenberg, W. Kohn, Inhomogeneous electron gas, Phys. Rev. 136 (1964).
[76] W. Kohn, L.J. Sham, Self-consistent equations including exchange and correlation effects, Phys. Rev. 140 (1965).
[77] E. Runge, E.K.U. Gross, Density-functional theory for time-dependent systems, Phys. Rev. Lett. 52 (1984) 997–1000.
[78] Xu Bu-Xing, A.K. Rajagopal, Current-density-functional theory for time-dependent systems, Phys. Rev. A 31 (1985) 2682.
[79] W. Kohn, Nobel lecture: Electronic structure of matter—wave functions and density functionals, Rev. Modern Phys. 71 (1998) 1253.
[80] J.P. Perdew, Density-functional approximation for the correlation energy of the inhomogeneous electron gas, Phys. Rev. B 33 (1986) 8822.
[81] C. Lee, W. Yang, R.G. Parr, Development of the Colle–Salvetti correlation-energy formula into a functional of the electron density, Phys. Rev. B 37 (1988) 785.
[82] K. Putteneers, F. Brosens, Monte-Carlo implementation of density-functional theory, Phys. Rev. B 86 (2012) 085115.
[83] L. Praxmeyer, J. Mostowski, K. Wodkiewicz, Hydrogen atom in phase space: The Wigner representation, J. Phys. A: Math. Gen. 39 (2006) 14143–14151.
[84] R.W. Hockney, J.W. Eastwood, Computer simulation using particles, A. Hilger (1988).
[85] A. Goldberg, H.M. Schey, Computer-generated motion pictures of one-dimensional quantum-mechanical transmission and reflection phenomena, Amer. J. Phys. 35 (1967) 177.
[86] J.M. Sellier, GNU Archimedes, www.gnu.org/software/archimedes, 2014 (accessed 24.06.14).